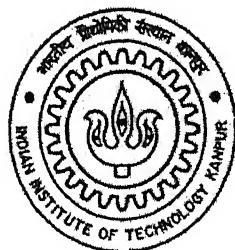


PARAMETER ESTIMATION OF A FLEXIBLE AIRCRAFT USING KALMAN FILTER ALGORITHM

A Thesis submitted
in partial fulfillment of the requirements
for the degree of
Master of Technology

by

A . Hari Gopal



to the

**Department of Aerospace Engineering
Indian Institute of Technology, Kanpur
India**

May, 2005.

११
५३/२०५/८
३६५८

१९ JUL 2005 / AE
दुर्घोत्तम कालिनार केन्द्र पुस्तकालय
भारतीय प्रौद्योगिकी संस्थान कानपुर
वराचि श. A...152192.....



A152192

CERTIFICATE

It is certified that the work contained in the thesis entitled "**PARAMETER ESTIMATION OF A FLEXIBLE AIRCRAFT USING KALMAN FILTER ALGORITHM**" by A.Hari Gopal has been carried out under my supervision and that this work has not been submitted elsewhere for a degree.

May, 2005.



(Dr. AJOY KANTI GHOSH)

Associate Professor
Department of Aerospace Engineering
Indian Institute of Technology
Kanpur - 208016

ABSTRACT

An attempt is made to estimate aerodynamic parameters using the simulated flight data of various flight vehicles using Kalman filter technique. The present thesis demonstrates application of Kalman filter for the estimation of ballistic coefficient of a falling body by considering the effects of process noise. The mathematical model of a flexible aircraft involves larger number of stability derivatives as compared to a rigid aircraft. Furthermore, for a flexible aircraft, additional derivatives need to be included due to aeroelastic effects. Applicability of Kalman filter for parameter estimation is validated on simulated flight data generated for a rigid aircraft as well as for a flexible aircraft. It is concluded that Extended Kalman Filter method can be advantageously applied to estimate aerodynamic parameters from flight data of a flexible aircraft.

ACKNOWLEDGEMENTS

With all humility and gratitude, I take this opportunity to express my sincere thanks to my teacher and thesis advisor, Dr Ajoy Kanti Ghosh for helping me in every possible way at all stages of this work. I am highly indebted to him for his genuine concern, active support and untiring interest.

I would like to thank with gratitude my lab mates Ankur Singhal, Mahender Kumar Samal, Sanjay Singh and Ujjwala for their cooperation and support during my thesis. My thanks to all my friends especially Abhiram, Amit, Bhavani, Kiran, K.S.V Reddy, Lovaraju, Rajarao, Ramanathan and Rupesh who encouraged me in times of need during my stay at IITK. I am also indebted to my senior K Venkat Chandra Sekhar whose valuable guidance helped me to complete this thesis.

A . Hari Gopal

Kanpur.

CONTENTS

Abstract	iii
List of figures	vii
List of tables	ix
Nomenclature	x
Chapter 1 Introduction	1
Chapter 2 Kalman Filter	9
2.1 Derivation of Scalar Riccati Equations	14
Chapter 3 Generation of flight data	17
3.1 Flight data of ballistic target (FD-BT)	17
3.2 Simulated Flight data of rigid aircraft (FD-RA/C)	20
3.3 Simulated Flight data of rigid aircraft (FD-AE A/C1 & FD-AE A/C2)	25
Chapter 4 Results and discussion	29
4.1 Estimation of Ballistic Coefficient from Flight Data Ballistic Target (FD-BT)	29
4.2 Estimation of Aerodynamic Parameters from Flight Data of Rigid Aircraft (FD-RA/C)	32
4.3 Estimation of 6 Aerodynamic Parameters from Flight Data of Flexible Aircraft (FD-AE A/C1 & FD-AE A/C2)	34
4.4 Estimation of 15 Aerodynamic Parameters from Flight Data of Flexible Aircraft (FD-AE A/C1 & FD-AE A/C2)	36

Chapter 5 Conclusion and suggestions for future work	40
5.1 Conclusion	40
5.2 Suggestions for future work	40
Appendix A	41
References	46

LIST OF FIGURES

Fig. No.	Title	Page No.
1.1	Filtering Approach	5
2.1	Power spectral density bandwidths	10
3.1	Radar tracking of ballistic target	18
3.2	Ballistic target trajectory for different β values	20
3.3	Simulated α response from the flight data FD-RA/C	22
3.4	Simulated q response from the flight data FD-RA/C	22
3.5	3-2-1-1 Elevator Control Input, $\delta_{\max} = 0.10471 \text{ rad}$	23
3.6	Simulated α response from the flight data FD-AE AC1 and FD-AE AC2	27
3.7	Simulated q response from the flight data FD-AE AC1 and FD-AE AC2	27
4.1	Estimation of ballistic coefficient β without process noise	30
4.2	Error in the estimation of ballistic coefficient β without Process noise	30
4.3	Estimation of ballistic coefficient β with process noise	31
4.4	Error in the estimation of ballistic coefficient β without Process noise	32
4.5	Comparison of the estimated α value with that of FD-RA/C	33
4.6	Comparison of the estimated q value with that of FD-RA/C	34
4.7	Comparison of the estimated α value with that of FD-AE A/C1	37
4.8	Comparison of the estimated q value with that of FD-AE A/C1	37
4.9	Comparison of the estimated α value with that of FD-AE A/C2	38

LIST OF TABLES

Table No.	Title	Page No.
3.1	Geometric, mass and aerodynamic characteristics of example aircraft	24
3.2	Vehicle Configuration	25
3.3	Aerodynamic Parameters of the flexible aircraft from Ref. 17	28
4.1	Estimated ballistic coefficient without process noise	29
4.2	Estimated ballistic coefficient with process noise	31
4.3	Estimated Aerodynamic Parameters from FD-RA/C	33
4.4	Equivalent aerodynamic parameters from FD-AE A/C1 and FD-AE A/C2	35
4.5	Estimated aerodynamic parameters from flight data FD-AE AC1 and FD-AE AC2	39

NOMENCLATURE

SYMBOLS:

C_m	Coefficient of pitching moment
C_L	Coefficient of Lift
C_{L0}	Coefficient of Lift at zero angle of attack
C_{m0}	Pitching moment coefficient of at zero angle of attack
c	Mean aerodynamic chord of example aircraft, m
S	Plan form area, m^2
g_B	Acceleration due to gravity, ft/s^2
g	Acceleration due to gravity, m/s^2
x	Altitude of ballistic target, ft
\dot{x}	Velocity of ballistic target, ft/s
\ddot{x}	Acceleration of ballistic target, ft/s^2
β	Ballistic coefficient, $\text{Lb}/\text{ft}/\text{s}^2$
C_{D0}	Coefficient of drag of ballistic target
$\hat{\rho}_B$	Density, Lb/ft^3
ρ	Density, kg/m^3
Q_p	Dynamic Pressure, $\text{Lb}/\text{ft}/\text{s}^2$
I_Y	Moment of inertia about y-axis of example aircraft, $\text{kg}\cdot\text{m}^2$
m	Aircraft mass, kg

W_B	Weight of ballistic target in Lb-ft/s ²
S_{ref}	Reference area of ballistic target, ft ²
M_i	Modal generalized mass
N	No state variables
η_i	Generalized displacement co-ordinate
$\dot{\eta}_i$	Derivative of generalized displacement coordinate
q	Pitch rate, rad/sec
\bar{q}	Dynamic Pressure, N/m ²
S	Reference wing area, m ²
t	Time, sec
u	velocity components along x axis, m/sec
ω_i	In vacuo frequency
α	Angle of attack, rad
δ, δ_e	Elevator deflection, rad
ζ	Structural damping ratio
x_n	aircraft motion variables
C_i	Aerodynamic Coefficient
U	Control inputs
\vec{x}	System space vector
\vec{z}	Measurement vector
$f(\vec{x})$	Nonlinear function of system states

$h(x)$	Nonlinear measurement function
w	Random zero mean process for process noise
v	Random zero mean process for measurement noise
$E()$	Expectation or mean
T_s	Sampling time
$[Q]$	Continuous process noise matrix
$[Q]_k$	Discrete process noise matrix
$[R]$	Measurement noise matrix
$[F]$	System dynamics matrix
$[H]$	Measurement matrix
$[\phi_k]$	Fundamental matrix
$[I]$	Identity matrix
$[P]$	Covariance matrix
$[K]$	Kalman gain matrix
F	System dynamics scalar
H	Measurement scalar
ϕ_k	Fundamental scalar
P	Covariance scalar
K	Kalman gain scalar

Superscripts

Derivative with respect to time

i, j General indices

\rightarrow Vector quantity

Subscripts

k After an update

$k-1$ Before an update

Abbreviations

FD-BT Flight Data of Ballistic Target

FD-AE AC1 Flight Data of Aeroelastic Aircraft with moderate flexibility

FD-AE AC2 Flight Data of Aeroclastic Aircraft with more flexibility

EKF Extended Kalman Filter

STABILITY AND CONTROL DERTIVATIVES

$$C_{L\alpha} = \partial C_L / \partial \alpha, \quad C_{Lq} = \partial C_L / \partial (qc/2u), \quad C_{L\delta_e} = \partial C_L / \partial \delta$$

$$C_{m\alpha} = \partial C_m / \partial \alpha, \quad C_{mq} = \partial C_m / \partial (qc/2u), \quad C_{m\delta_e} = \partial C_m / \partial \delta$$

CHAPTER 1

Introduction

All modern aerospace vehicles rely upon an understanding of dynamics and control to improve system performance. Successful system design requires an understanding of dynamic elements and the trade-off between vehicle dynamic characteristics, control system properties and system performance. Aircraft parameter estimation is one of the most outstanding and illustrated example of the system identification methodologies. The success of the system identification of the flight vehicle has been possible due to better measurement techniques and data processing capabilities provided by digital computers. Other factors that contribute to system identification are the developments in the fields such as estimation and control theory; the well understood basic principles of aerodynamic modeling and design of appropriate flight tests^{1,2,3}.

The equations of motion of early flight vehicles are derived from Newtonian mechanics, usually assuming flight vehicles to be rigid. Out of the various forces and moments (aerodynamic, inertial, gravitational and propulsive) acting on a flight vehicle, the determination of aerodynamic forces and moments presents the most difficult challenge till date. Flight vehicle identification of high performance and highly augmented vehicles include nonlinearities affected by elastic modes, unsteady aerodynamics and erroneous data measurements.

The concept of aircraft aerodynamic modeling was introduced by Bryan⁴, who provided relationship between the forces along the three Cartesian axes and the three

moments about these axes as a function of linear translational motion variables and rotational rates. The most commonly employed aerodynamic models are typically formulated as truncated Taylor-series expansion of the form

$$C_i = \sum_i \frac{\partial C_i}{\partial x_n} x_n + \sum_i \frac{\partial C_i}{\partial U} U : i=X, Y, Z, l, m, n \quad (1.1)$$

where x_n are the aircraft motion variables (angle-of-attack, angle of sideslip, airspeed, angular rates, etc.) and U are the inputs (control surface deflection, etc.). X, Y, Z are the forces and l, m, n are the moments about x, y and z axes respectively. However, such aerodynamic model structures can be surprisingly deceptive to their actual complexity. Some of the models postulated contain large number of parameters including two dimensional functions, acceleration derivatives, derivatives due to elastic modes, etc. The increase in the size of model structure makes the evaluation of the suitability of the model much more difficult.

After a priori fix of the aerodynamic model, the next task of estimating parameters (stability and control derivatives) has been attempted by three different but complimentary techniques: analytical methods, wind tunnel methods, and flight – test methods. At the initial stages of aircraft design, analytical methods provide the only convenient way of estimating the aircraft parameters. However, the accuracy of such theoretical estimates being not so high, there is need to verify these estimates with those obtained from wind tunnel testing and flight testing. In recent years, computational fluid dynamics (CFD) has contributed positively towards analytical estimation of aerodynamic coefficients by way of numerical solutions of total configuration via sophisticated and advanced Euler and Navier – Stokes flowsolvers⁵. Nevertheless, experimental methods are essential to corroborate the analytical predictions. Although wind tunnel methods

improve the accuracy of estimation of parameters, they are time consuming and expensive. Furthermore, simulation of control surfaces, power effects and stringent flight conditions are difficult to simulate satisfactorily. Wind-tunnel estimates also suffer discrepancies due to interference effects of support systems, wall effects, turbulence level, etc. It is, therefore, desirable that the wind tunnel estimates be corroborated with the estimates from actual flight test data.

One of the first attempts to obtain static and dynamic parameters from flight data was in 1947 by Milliken⁶. Using semi-graphical method, he analyzed the frequency response data for obtaining the characteristics of the short period longitudinal motion of the aircraft. Later, Shinbrot⁷ proposed more general and rigorous methods based on application of ordinary and nonlinear least squares, for estimating parameters from transient maneuvers. In the late sixties and early seventies, the proliferation of high-speed, general purpose digital computers gave a new impetus to the development of more sophisticated, elegant and innovative identification techniques. The bulk of information on general identification theory and its dynamics have been documented in several reports and survey papers. A systematic discussion on the chronological evolution of flight vehicle system identification starting from determination of aircraft frequency and damping ratio from flight data in early twenties to the present day advanced applications is given in a survey paper of Hamel and Jategaonkar⁵.

The most commonly used methods to estimate stability and control derivatives from flight data are broadly classified into the following categories.

- Equation error methods
- Output error methods

- Filtering approach
- Filter-error methods

The principle of least squares⁸ is used in the equation error method wherein the error gets minimized with respect to the unknown parameters in each of the equations. Its advantages include computational simplicity, non-iterative nature and applicability to both linear and non-linear models. The disadvantage is that the method cannot be directly applied if all the states are not measured accurately, and produces poor results if the measurements are noisy. Therefore in order to get accurate results, considerable effort is required for data reconstruction and smoothing. Sometimes these data processing tasks are more complicated than the task of parameter estimation itself. However these methods are useful as startup for more advanced estimators.

In the output error method, the error between the measured and the model response is minimized. The method assumes that there exist no modeling errors. This method processes the measurement noise while assuming the model representation of the given system to be exact. A comprehensive survey of these methods is reported by Maine and Iliff². The methods like analog matching⁹, Newton Raphson method¹⁰, modified Newton Raphson method¹⁰ etc. fall in this category. Maximum likelihood (ML)⁵ method is one of the variants of output error methods. Maximum Likelihood estimates are those for which the observed value would be the most likely to occur; “most likely” is defined as maximization of likelihood function of the observed responses, given the parameters. The main advantage of this method is that parameter estimates are asymptotically unbiased, consistent and efficient provided the model assumed is correct.

Kalman filter^{8,11,12} is a linear, optimal estimator of state variables of a linear, time-varying system, operating in a Gaussian stochastic environment. Filtering approach^{5,13} is an extension of Kalman filter. Optimal estimator here is referred to a computational algorithm that processes measurements to deduce a minimum error covariance of the state of a system combining all the information available.

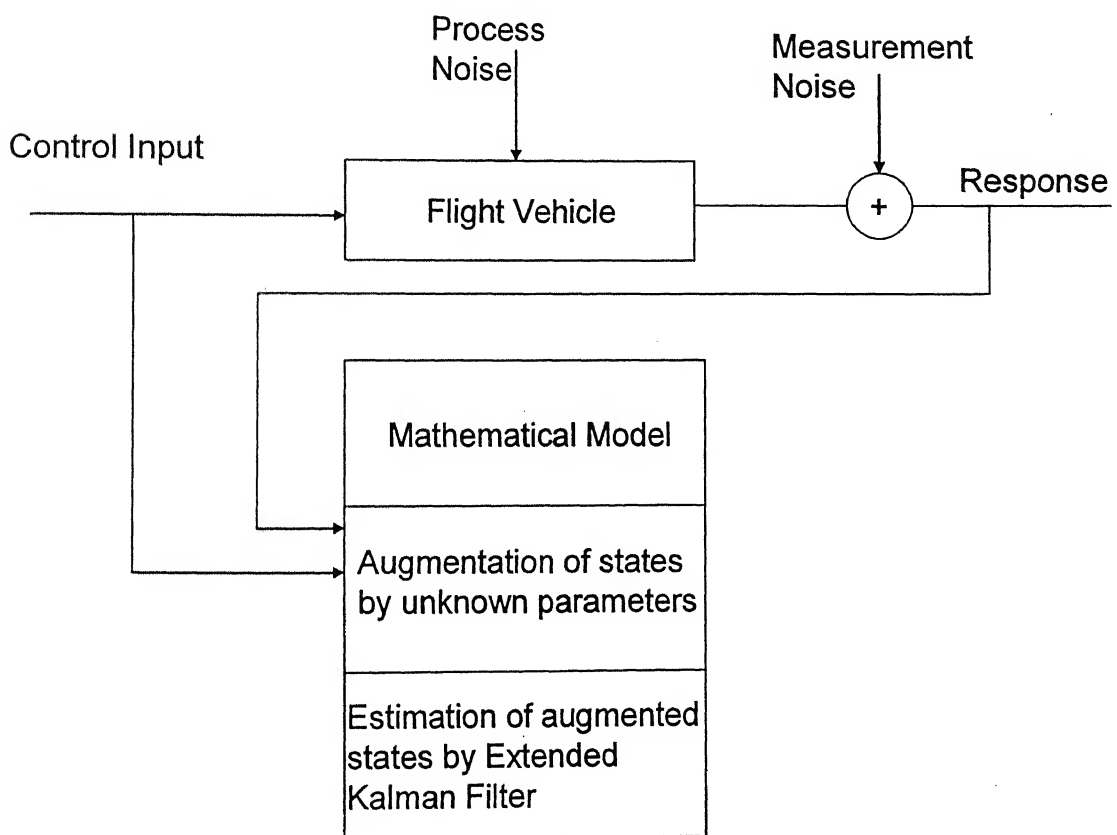


Fig. 1.1 Filtering Approach

Generally, Kalman filter^{13,14} is applicable and optimal for linear systems only. When either the system or the measurement equations are non-linear, the same algorithm can still be applied by local linearization of the system about the current state. Such filter applied to nonlinear systems is called Extended Kalman Filter (EKF)¹⁵, and it need not be optimal. EKF produces estimates of the parameters that approximately minimize the

mean square error in the parameter estimates themselves as opposed to ML and least squares which minimize a cost function that is based on matching the output variable behavior given a specific input trajectory. The filtering approach as presented pictorially in Fig. 1.1 is well suited for online applications and can handle process noise (modeling errors) and measurement noise (instrument errors). Extended Kalman Filter produces time histories for each of the estimated parameters, which is very useful if the time-varying nature of the parameters is of interest. But the performance of the filter strongly depends on the initial statistics of process noise, measurement noise and a priori covariance matrix. Information about the measurement noise covariance can be obtained from the laboratory calibration of measurement sensors used. Process noise is however more difficult to determine. Several procedures for obtaining measurement and process noise prior to estimation are available in literature. Well known methods by Mehra¹⁴ and Morelli¹⁵ are being used with partial success. Other kind of approach known as adaptive filtering adjusts the variances during the estimation of parameters. Myers and Tapley¹⁶ gave one such algorithm of adaptive filtering/tuning. In the present work no attempt has been made to use adaptive filtering technique.

Filter error method^{5,13} is the most general stochastic approach to parameter estimation, which accounts for both process and measurement noise. It can give good estimates from data collected in turbulent atmosphere (process noise) also. In this direct approach an appropriately defined cost function, usually the statistically formulated likelihood function, is optimized with respect to the unknown parameters using some suitable optimization method. The Gauss Newton method is generally used for this

purpose. Filter is used only for the natural purpose of obtaining the true state variables from the noisy measurements, i.e. for state estimation.

Parameter estimation of an aircraft with many measurements like, acceleration (both linear and angular), angular orientation, speed, angle of attack etc. has been discussed in detail in Ref..5. But from cost effectiveness point of view, it may not be feasible to use many sensors for air borne vehicles that go through many development trials.

In the present work, EKF method is used for parameter estimation from flight data of air borne vehicles. The motivation here was to conduct a study on the applicability of the method in extracting aerodynamic parameters by processing flight data obtained for different class of flight vehicle/store. The method has been applied to flight data of a one-dimensional ballistic target, flight data of a rigid aircraft in longitudinal short period mode and also to flight data of a flexible aircraft in longitudinal short period mode. Any parameter estimation method requires adequate information about vehicle dynamics to estimate aerodynamic parameters correctly. Flight data of one-dimensional ballistic target contains very limited information regarding its motion/control variables. The flight data obtained through aircraft maneuvers contains more information regarding its motion and control variables. The applicability of the EKF is tested for these three different classes of flight data. It is observed that EKF can be advantageously applied on flight data of flexible aircraft to estimate few aerodynamic parameters with acceptable level of accuracy.

Chapter 2 describes the description of Kalman filter and the mathematics involved in the filter design. Chapter 3 presents methodologies used to generate flight data for

different type of vehicles considered. In chapter 4 results and discussions are presented and chapter 5 concludes with scope for future work.

CHAPTER 2

Kalman Filter

Kalman filter is an optimal recursive data processing algorithm and it incorporates all information that is available to the filter. It processes all available measurements, regardless of their precision, to estimate the current values of the variables of interest with use of

- knowledge of the system and measurement device dynamics
- the statistical description of the system noises, measurement errors, and uncertainty in the dynamic models
- any available information about initial conditions of the variables of interest

This filter performs the conditional probability density propagation for problems in which the system can be described through a linear model and in which system and measurement noises are white and Gaussian. The three basic assumptions in Kalman filter formulation are

- the model is considered to be linear .
- the measurement noise and system noise are white.
- the measurement noise and system noise are Gaussian.

The physical implications of these assumptions are discussed. A linear model is justifiable because when nonlinearities do exist, the typical engineering approach is to linearize about some nominal point or trajectory, achieving a perturbation model or error model.

“Whiteness” implies that the noise value is not correlated in time. The knowledge of the present noise value is no way helpful to predict the noise value of any other time. Whiteness also implies that the noise has equal power at all

frequencies. A system will be driven by a wideband noise, noise having power at all frequencies above the system bandpass and essentially constant power at frequencies within the system bandpass. The assumption of noise as white would extend this constant power level out across all frequencies.

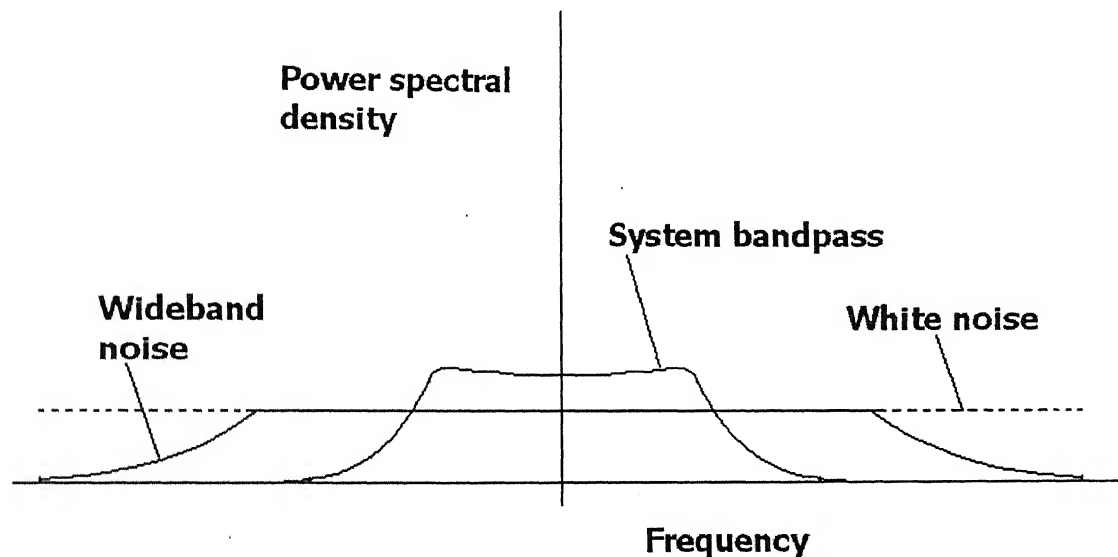


Fig. 2.1 Power spectral density bandwidths

Within the bandpass of the system of interest, the fictitious white noise looks identical to the real wideband noise. The mathematics involved in the filter are vastly simplified by replacing the real wideband noise with a white noise which from the system's "point of view" is identical. Gaussianness is related with amplitude whereas whiteness is related with frequency. The probability density of Gaussian noise amplitude takes on the shape of a normal bell -shaped curve. This assumption is justified physically by the fact that a system or measurement noise is typically caused by a number of small sources. Mathematically, when a number of independent random variables are added together, the summed effect can be described very closely by a Gaussian probability density, regardless of the shape of the individual densities.

The first and second order statistics (mean and variance or standard deviation) of a noise process can be easily known. In the absence of any higher order statistics, there is no better form to assume than the Gaussian density. The first and second order statistics completely determine a Gaussian density, unlike most densities which require endless number of orders of statistics to specify their shape entirely. The Kalman filter, which propagates the first and second order statistics, includes all information contained in the conditional probability density.

The real world situation is described by a set of nonlinear differential equations to apply extended Kalman filter techniques. These equations are expressed in nonlinear state-space form as a set of first-order non linear differential equations as

$$\dot{x} = f(\bar{x}) + w \quad (2.1)$$

where ' \dot{x} ' represents system space, ' $f(\bar{x})$ ' is a nonlinear function of those states and ' w ' is a random zero-mean process. The continuous process-noise matrix describing the random process w for the preceding model is given by

$$[Q] = E(ww^T) \quad (2.2)$$

The measurement equation, required for the application of extended Kalman filtering, is considered to be a nonlinear function of the states according to the equation

$$\bar{z} = h(x) + v \quad (2.3)$$

where ' v ' is a zero-mean random process described by the measurement noise matrix [R], which is defined as

$$[R] = E(vv^T) \quad (2.4)$$

For systems in which the measurements are discrete, the nonlinear measurement equation is written as

$$\bar{z}_k = h(\bar{x}_k) + v_k \quad (2.5)$$

The discrete measurement noise matrix $[R]_k$ consists of a matrix of variances representing each measurement noise source. Since, the system equation, Eq. 2.1 and measurement equation, Eq 2.3 are nonlinear, a first order approximation is used in the continuous Riccati equations for the manipulation of systems dynamics matrix $[F]$ and the measurement matrix $[H]$. The matrices are related to the nonlinear system and measurement equations according to the relations

$$[F] = \left. \frac{\partial f(x)}{\partial x} \right|_{x=\hat{x}} \quad (2.6)$$

$$[H] = \left. \frac{\partial h(x)}{\partial x} \right|_{x=\hat{x}} \quad (2.7)$$

The fundamental matrix $[\phi_k]$, required for the discrete Riccati equations, can be approximated by the Taylor-series expansion for $\exp([F] T_s)$ and is given by the equation

$$[\phi]_k = [I] + [F]T_s + \frac{[F]^2 T_s^2}{2!} + \frac{[F]^3 T_s^3}{3!} + \dots \quad (2.8)$$

where ' T_s ' is the sampling time and $[I]$ is the identity matrix. In our applications of extended Kalman filtering, the series is approximated by only the first two terms, because $[\phi]_k$ is only used for the calculation of Kalman gains and the matrix may not necessarily improve the performance of the filter by considering more terms. Therefore $[\phi]_k$ is given by

$$[\phi]_k \approx [I] + [F]T_s \quad (2.9)$$

The matrix Riccati equations, required for the computation of the Kalman gains, are given by the equations

$$[M]_k = [\phi]_k [P]_{k-1} [\phi]_k^T + [\mathcal{Q}]_k \quad (2.10)$$

$$[K]_k = [M]_k [H]^T \left([H][M]_k [H]^T + [R]_k \right)^{-1} \quad (2.11)$$

$$[P]_k = ([I] - [K]_k [H]) [M]_k \quad (2.12)$$

where $[P]_k$ is the covariance matrix representing errors in the state estimates after an update, $[K]_k$ is the Kalman gain and $[M]_k$ is the covariance matrix representing errors in the state estimates before an update. The discrete process-noise matrix $[\mathcal{Q}]_k$ can be found from the continuous process-noise matrix according to equation

$$[\mathcal{Q}]_k = \int_0^{T_s} [\phi(\tau)] [\mathcal{Q}] [\phi(\tau)]^T d\tau \quad (2.13)$$

The preceding approximations for the fundamental and measurement matrices are used in the computation of the Kalman gains. The new state estimate \hat{x}_k is the old state estimate \bar{x}_{k-1} projected forward to the new sampling \bar{x}_k plus a gain times a residual. The residual is the difference between the actual measurement z_k and the nonlinear measurement $h(\bar{x}_k)$.

$$\hat{x}_k = \bar{x}_k + K_k [z_k - h(\bar{x}_k)] \quad (2.14)$$

The old estimates that have to be propagated forward do not have to be done with the fundamental matrix but instead can be propagated directly integrating the actual nonlinear differential equations forward at each sampling interval. Euler integration is applied to the nonlinear system of differential equations and is given by the equation

$$\bar{x}_k = \hat{x}_{k-1} + \hat{x}_{k-1} T_s \quad (2.15)$$

where the derivative is obtained from

$$\hat{x}_{k-1} = f(\hat{x}_{k-1}) \quad (2.16)$$

In the preceding equation the sampling time T_s is used as an integration interval. In the problems where the sampling time is large, T_s would have to be replaced by a small integration interval, or possibly a more accurate method of integration has to be used.

Derivation of Scalar Riccati Equations

When there is no deterministic disturbance or control scalar the discrete model is given by

$$x_k = \phi_k x_{k-1} + w_k \quad (2.17)$$

where ' ϕ_k ' is the scalar that propagates the states from one sampling instant to the next and ' w_k ' is the white process noise. The scalar Kalman – filtering equation for this discrete model is

$$\hat{x}_k = \phi_k \hat{x}_{k-1} + K_k (z_k - H\phi_k \hat{x}_{k-1}) \quad (2.18)$$

The measurement scalar equation is given by

$$z_k = Hx_k + v_k \quad (2.19)$$

where ' H ' is the measurement scalar that relates the state to measurement and ' v_k ' is the measurement noise. The error in the estimate at time ' k ' is given by this equation

$$\tilde{x}_k = x_k - \hat{x}_k = x_k - \phi_k \hat{x}_{k-1} + K_k (z_k - H\phi_k \hat{x}_{k-1}) \quad (2.20)$$

Substituting Eq. 2.17 and Eq. 2.19 in the Eq. 2.20 yields the following equation

$$\tilde{x}_k = \phi_k x_{k-1} + w_k - \phi_k \hat{x}_{k-1} - K_k (H\phi_k x_{k-1} + Hw_k + v_k - H\phi_k \hat{x}_{k-1}) \quad (2.21)$$

The error at time ' $k-1$ ' is given by the equation

$$\tilde{x}_{k-1} = x_{k-1} - \hat{x}_{k-1} \quad (2.22)$$

Combining similar terms of the Eq. 2.21 yields

$$\tilde{x}_k = (1 - K_k H) \tilde{x}_{k-1} \phi_k + (1 - K_k H) w_k - K_k v_k \quad (2.23)$$

P_k , Q_k and R_k are defined as covariance scalar, process noise scalar and measurement noise scalar respectively and are computed by the expectations of square of the error in the estimate, square of the process noise and square of the measurement noise respectively as follows

$$P_k = E(\tilde{x}_k) \quad (2.24)$$

$$Q_k = E(w_k^2) \quad (2.25)$$

$$R_k = E(v_k^2) \quad (2.26)$$

Squaring and taking expectations of the Eq. 2.23 yields

$$P_k = (1 - K_k H)^2 (P_{k-1} \phi_k^2 + Q_k) + K_k^2 R_k \quad (2.27)$$

since the process noise and measurement noise are considered to be zero mean noise their expectations are zero.

The Eq. 2.27 can be further simplified by defining a term M_k as

$$M_k = P_{k-1} \phi_k^2 + Q_k \quad (2.28)$$

Eq. 2.28 is analogous to the Riccati first equation, Eq. 2.10 and on substitution of Eq. 2.28 in Eq. 2.27 the equation simplifies to

$$P_k = (1 - K_k H)^2 M_k + K_k^2 R_k \quad (2.29)$$

The optimal gain that will minimize the variance of the error in the estimate is obtained by equating the derivative of P_k with respect to Kalman gain, K_k to zero.

$$\frac{\partial P_k}{\partial K_k} = 0 \quad (2.30)$$

$$2(1 - K_k H) M_k (-H) + 2K_k R_k = 0 \quad (2.31)$$

The Kalman gain, K_k is given by the expression

$$K_k = \frac{M_k H}{H^2 M_k + R_k} = M_k H (H^2 M_k + R_k)^{-1} \quad (2.32)$$

Eq. 2.32 is analogous to the second Riccati equation, Eq. 2.11. Substitution of the optimal gain K_k in the Eq. 2.29 yields,

$$P_k = \left(1 - \frac{M_k H^2}{H^2 M_k + R_k}\right) M_k + \left(\frac{M_k H}{H^2 M_k + R_k}\right)^2 R_k \quad (2.33)$$

The Eq. 2.33 is simplified further by the use of Eq. 2.32 to

$$P_k = \frac{R_k M_k}{H^2 M_k + R_k} = \frac{R_k K_k}{H} \quad (2.34)$$

Rearranging the optimal gain equation, Eq. 2.32

$$K_k R_k = M_k H - H^2 M_k K_k \quad (2.35)$$

Substituting Eq. 2.35 in Eq. 2.34 yields

$$P_k = \frac{M_k H - H^2 M_k K_k}{H} = (1 - K_k H) M_k \quad (2.36)$$

Eq. 2.36 is analogous to the third Riccati equation, Eq. 2.12. These three Riccati equations are simply an iterative way of finding the optimal gain at each time step. The matrix Riccati equations also resemble the scalar Riccati equations and their derivation is far more complex than the scalar derivation and is not mentioned in the present work.

CHAPTER 3

Generation of Flight Data

Due to the non-availability of real flight data, simulated flight data is generated for different class of flight vehicles for the purpose of parameter estimation. Mathematical models used to generate flight data of ballistic target (FD-BT), longitudinal motion of rigid aircraft (FD-RA/C) and longitudinal motion of flexible aircraft (FD-AE A/C1, FD-AE A/C2) are presented in subsequent paragraphs. For the generation of simulated flight data of ballistic target the acceleration equation governing the path of the trajectory was solved using Euler integration. In the case of aircraft, longitudinal equations of motion were solved using fourth-order Runge -Kutta method. Subsequently, the simulated flight-data of the air borne vehicles is used in Kalman filter algorithm and processed for the estimation of aerodynamic parameters. The equations of motion are needed for generating the simulated flight data and also in the Kalman filter algorithm for the propagation of states from one time step to the other.

Flight Data of Ballistic Target (FD-BT)⁸

Knowledge of target ballistic coefficient is used in advance guidance laws such as predictive guidance to relax the interceptor acceleration requirements. In addition, knowledge of the target ballistic coefficient is required for fire control due to the importance of accurate intercept point predictions in launching the interceptor on a collision course. Therefore, accurate estimation of ballistic coefficient of a target re-entering the atmosphere is very important for both guidance and fire control purposes.

The flight data for simulating such a vehicle motion is modeled to investigate the applicability of EKF method⁸ in extracting parameter (ballistic coefficient) from flight data.

The one-dimensional example of a ballistic target falling on tracking radar is considered. The target was initially at 2, 00,000 ft above the radar and had a velocity of 6000 ft/s towards the radar, which is located in the surface of a flat Earth. The trajectory of the ballistic target is presented in Fig. 3.2. The radar measures the altitude of the target with 25-ft standard deviation measurement accuracy. The radar picks measurements for every 0.1-sec. The simulation is done for 30 sec. An extended Kalman filter is built to estimate the altitude, velocity and ballistic coefficient.

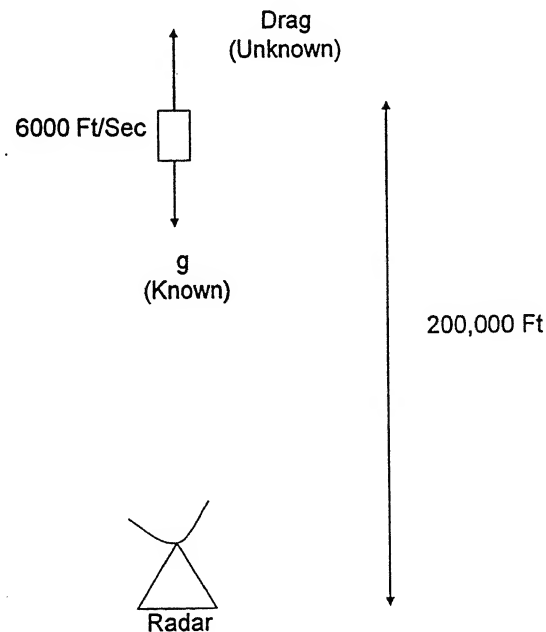


Fig. 3.1 Radar tracking of ballistic target .

The two forces acting on the object are the drag force and the gravity force. The equation that governs the motion of the object is given by

$$\ddot{x} = \frac{Q_p g_B}{\beta} - g_B \quad (3.1)$$

where ' \ddot{x} ' is the acceleration acting on the object, ' g_B ' is the acceleration due to gravity and ' Q_p ' the dynamic pressure and is given by the equation

$$Q_p = 0.5 \hat{\rho}_B \dot{x}^2 \quad (3.2)$$

where ' \dot{x} ' is the velocity of the target and the air density ' ρ_B ' in Eq. (3.2) is an exponential function of altitude and is given by the equation

$$\hat{\rho}_B = 0.0034 e^{-x/22000} \quad (3.3)$$

The term ' β ' in Eq. (3.1) is the ballistic coefficient and is expressed as

$$\beta = \frac{W_B}{S_{ref} C_{D0}} \quad (3.4)$$

where ' W_B ' is the weight of the ballistic target, ' S_{ref} ' is the reference area of the object and ' C_{D0} ' is the coefficient of drag. The acceleration acting on the object is expressed as the nonlinear second order differential equation as

$$\ddot{x} = \frac{0.0034 g_B e^{-x/22000}}{2\beta} - g_B \quad (3.5)$$

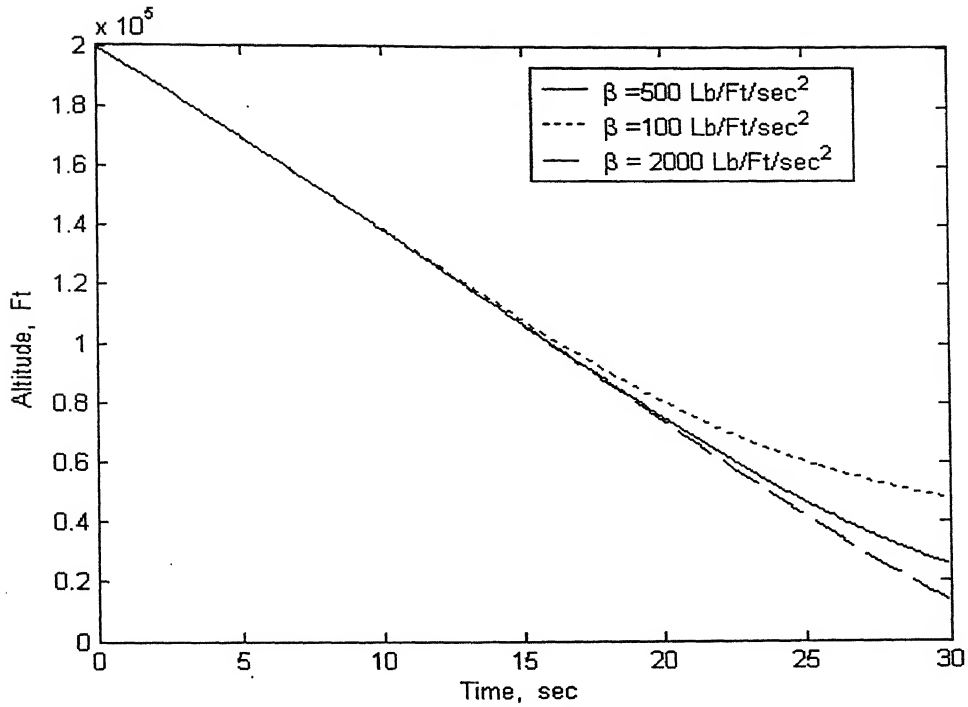


Fig. 3.2 Ballistic target trajectory for different β values

The procedure of application of Kalman filter algorithm for the case of Ballistic Target is explained in Appendix -A.

Simulated Flight Data of Rigid Aircraft(FD-RA/C):

In most cases, longitudinal maneuvers predominantly excite the short period mode and not the phugoid mode. In short period mode the flight velocity is essentially constant during the maneuver. 3-2-1-1 control (elevator) input is considered for the excitation of short period mode. The example aircraft mentioned in Ref. 17 was chosen for the present study. The mass, geometric and aerodynamic characteristics of this example aircraft are presented in Table 3.1. Trim flight conditions correspond to straight and level cruise flight at an altitude of 1500m and at a Mach number of 0.6. The rigid body short period longitudinal response to a given elevator input was simulated for 8

seconds. The short period longitudinal response was simulated using the following equations.

$$\dot{\alpha} - q = - \rho u S C_L / 2m \quad (3.6)$$

$$\dot{q} = \rho u^2 S c C_m / 2 I_Y \quad (3.7)$$

The equations that define coefficient of lift (C_L) and pitching moment coefficient (C_m) in Eq. (3.6) and Eq. (3.7) to describe the aerodynamic model are presented in Eq. (3.8) and Eq. (3.9)

$$C_L = C_{L0} + C_{L\alpha} \alpha + C_{Lq} \frac{q \bar{c}}{2u} + C_{L\delta_e} \delta_e \quad (3.8)$$

$$C_m = C_{m0} + C_{m\alpha} \alpha + C_{mq} \frac{q \bar{c}}{2u} + C_{m\delta_e} \delta_e \quad (3.9)$$

The pitching moment coefficient (C_m) is with reference to the center of gravity. The Eq. (3.6) and Eq. (3.7) were solved using fourth-order Runge-Kutta algorithm with a time step of 0.001 sec to obtain simulated flight data. The contribution due to aeroelastic effect was neglected for rigid aircraft case. The flight data used for parameter estimation is pictorially presented in Fig. 3.3 and Fig. 3.4. This flight data will be referred to as FD-RAC for further purpose. The elevator input (3-2-1-1) used to generate this flight data is shown in Fig. 3.5.

त्रिशोल्म काणीनाथ केलकर पुस्तकालय
भारतीय प्रौद्योगिकी संस्थान कानपूर
मवाप्ति क्र. A 152192....

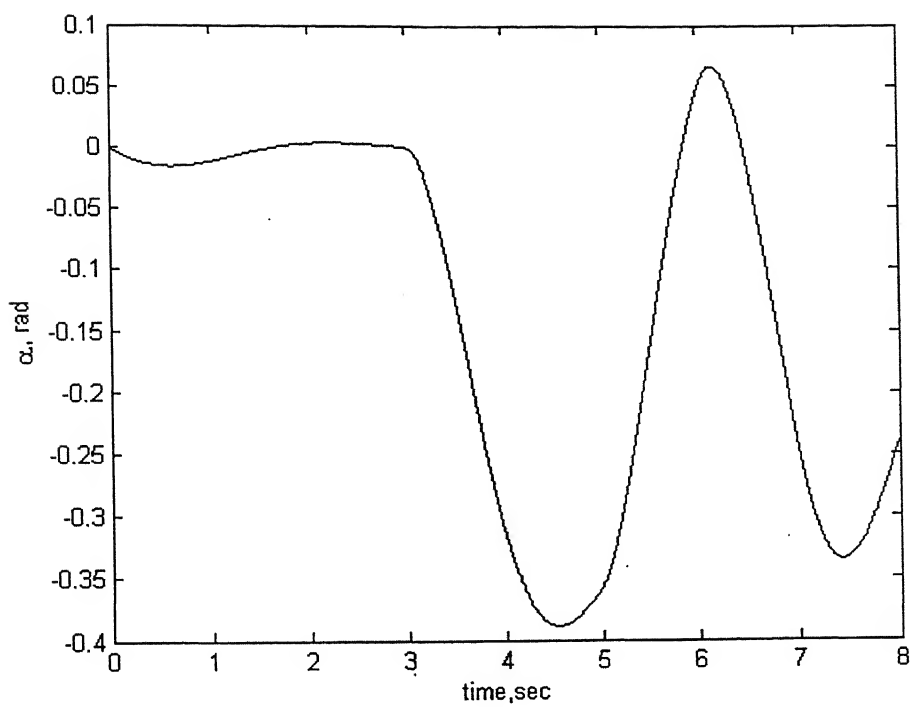


Fig. 3.3 Simulated α response from the flight data FD-RA/C

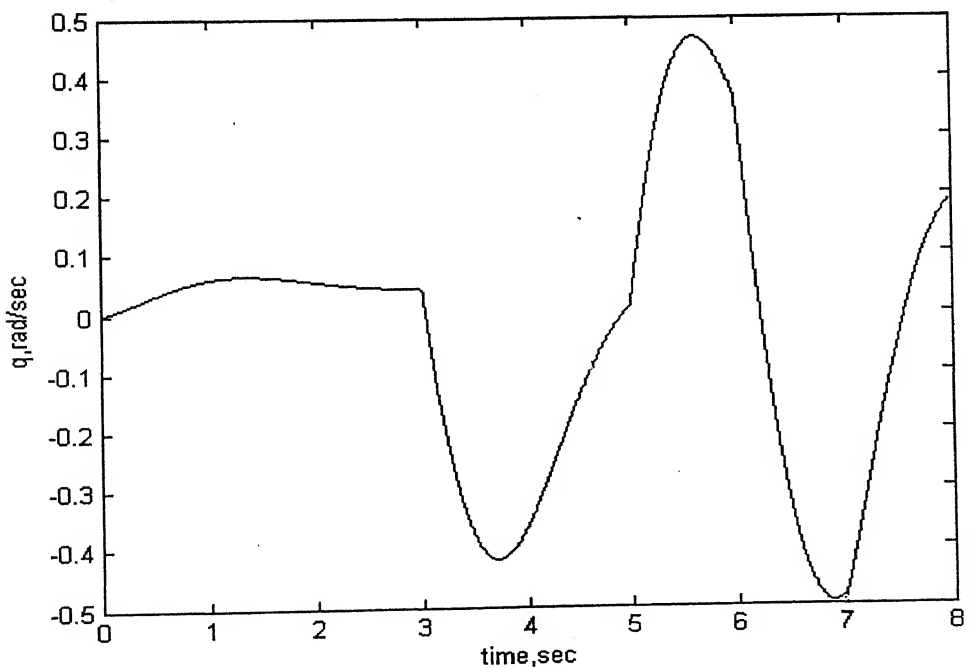


Fig. 3.4 Simulated q – response from flight data FD-RA/C

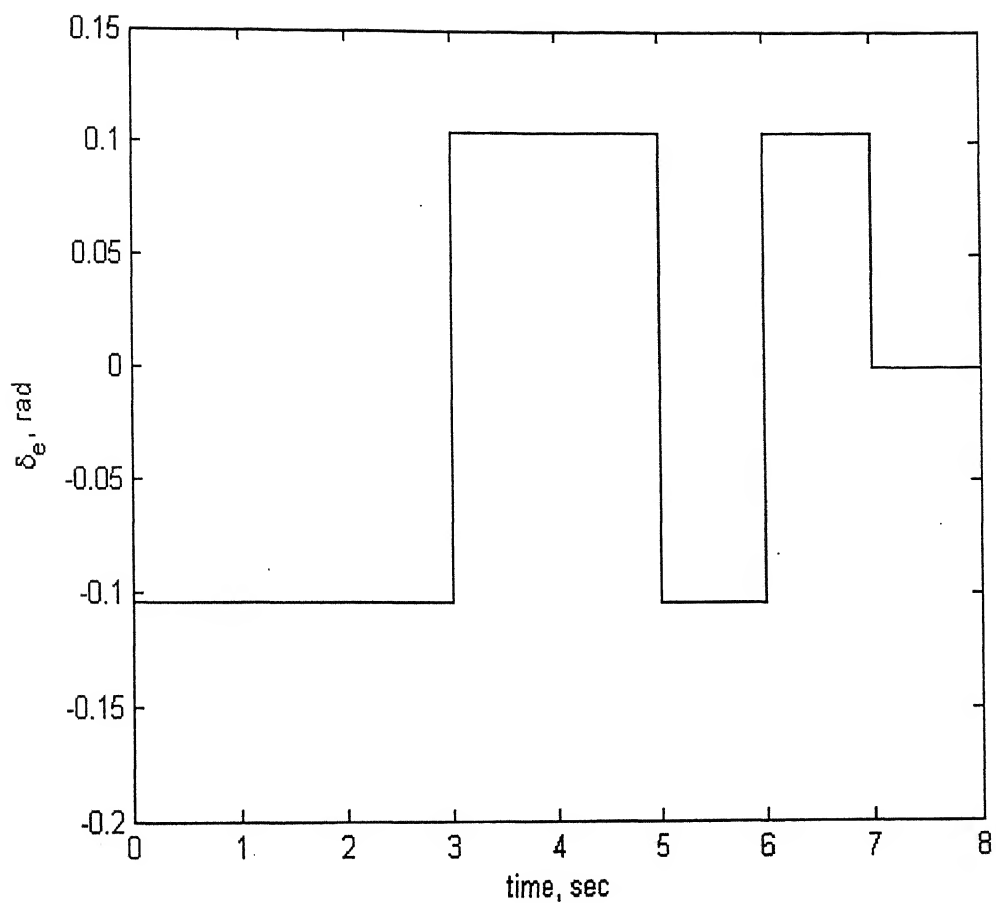


Fig. 3.5 3-2-1-1 Elevator Control Input, $\delta_{\max} = 0.10471 \text{ rad}$

Table 3.1 Geometric, mass and aerodynamic characteristics of example aircraft

Mean Chord	$c = 4.663 \text{ m}$
Wing Sweep	$\Lambda = 65^\circ$
Wing Area	$S = 180.79 \text{ m}^2$
Mass	$m = 130642.31 \text{ kg}$
Moment of Inertia about Y axis	$I_Y = 8677231.17 \text{ kg-m}^2$
	$M_1 = 248.86 \text{ kg-m}^2$
Modal generalized masses	$M_2 = 12984.23 \text{ kg-m}^2$
	$M_3 = 1807.34 \text{ kg-m}^2$
	$M_4 = 59048.57 \text{ kg-m}^2$
Aerodynamic Parameters	
C_{L0}	0.34
$C_{L\alpha}$	2.9223
C_{Lq}	-14.7
$C_{L\delta_e}$	0.43548
C_{m0}	-0.252
$C_{m\alpha}$	-1.6617
C_{mq}	-34.75
$C_{m\delta_e}$	-2.578

Table 3.2 Vehicle Configuration

Configuration	In vacuo modal frequencies ω_i (rad/s)			
	Mode 1	Mode 2	Mode 3	Mode 4
AE A/C1	12.57	14.07	21.17	22.05
AE A/C2	6.29	7.04	10.59	11.03

Simulated Flight Data of Flexible Aircraft FD-AE A/C1 & FD-AE A/C2)

The non linear equations of motion for a flexible aircraft are considered which are obtained from Ref. 17.

$$\dot{\alpha} - q = -\rho u S / 2m \left[C_{L0} + C_{L\alpha} \alpha + C_{Lq} \frac{q \bar{c}}{2V} + C_{L\delta_e} \delta_e + \sum_{i=1}^n (C_{L\eta_i} \eta_i + C_{L\dot{\eta}_i} \dot{\eta}_i c / 2u) \right] \quad (3.10)$$

$$\dot{q} = \rho u^2 Sc / 2I_Y \left[C_{m\alpha} \alpha + C_{mq} q c / 2u + C_{m\delta_e} \delta_e + \sum_{i=1}^n (C_{m\eta_i} \eta_i + C_{m\dot{\eta}_i} \dot{\eta}_i c / 2u) \right] \quad (3.11)$$

where angle of attack α , pitch rate q and control input δ_e represent the perturbations and η_i and $\dot{\eta}_i$ are the generalized displacement coordinates and their derivatives. $C_{L\alpha}$, C_{Lq} , $C_{L\delta_e}$, $C_{m\alpha}$, C_{mq} , $C_{m\delta_e}$, $C_{L\eta_i}$, $C_{L\dot{\eta}_i}$, $C_{m\eta_i}$ and $C_{m\dot{\eta}_i}$ are the aerodynamic coefficients as defined in Ref. 17. The second order differential equation that is satisfied by the generalized displacement coordinates and its derivatives is taken from Ref. 17 and is given in Eq. 3.12. The additional term $2\xi_i \omega_i \eta_i$ representing the structural damping is also included.

$$\ddot{\eta}_i + 2\xi_i \omega_i \dot{\eta}_i + \omega_i^2 \eta_i = \rho u^2 Sc / 2M_i \left[C_{\alpha}^{\eta_i} \alpha + C_q^{\eta_i} qc / 2u + C_{\delta}^{\eta_i} \delta + \sum_{j=1}^n \left(C_{\eta_j}^{\eta_i} \eta_j + C_{\dot{\eta}_j}^{\eta_i} \dot{\eta}_j c / 2u \right) \right] \quad (3.12)$$

where ω_i , ξ_i and M_i are the in-vacuo frequency, modal damping, and modal generalized mass respectively and $C_{\alpha}^{\eta_i}$, $C_q^{\eta_i}$, $C_{\delta}^{\eta_i}$, $C_{\eta_j}^{\eta_i}$ and $C_{\dot{\eta}_j}^{\eta_i}$ represent the generalized force derivatives due to coupling in elastic and aerodynamic degrees of freedom. Eq. 3.10, Eq. 3.11 and Eq. 3.12 are integrated to generate motion variables α and q . The elevator control input is 3-2-1-1 and is presented in Fig. 3.5. The aerodynamic model incorporating aeroelastic effects is presented in Eq.(3.13) and Eq.(3.14)

$$C_L = C_{L0} + C_{L\alpha} \alpha + C_{Lq} qc / 2u + C_{L\delta_e} \delta_e + \sum_{i=1}^4 \left[C_{L\eta_i} \eta_i + (C_{L\dot{\eta}_i} \dot{\eta}_i) c / 2u \right] \quad (3.13)$$

$$C_m = C_{m0} + C_{m\alpha} \alpha + C_{mq} qc / 2u + C_{m\delta_e} \delta_e + \sum_{i=1}^4 \left[C_{m\eta_i} \eta_i + (C_{m\dot{\eta}_i} \dot{\eta}_i) c / 2u \right] \quad (3.14)$$

The numerical values of the aerodynamic parameters are listed in Table 3.3. The flight data obtained for this case is pictorially presented in Fig. 3.6 and Fig. 3.7. To study the effect of flexibility of the structure on parameter estimation, two cases are considered. The two set of modal frequencies for the two different configurations are listed in Table 3.2. To start with aircraft with moderate flexibility is considered. The flight data obtained with this case will be referred to as FD-AE A/C. In the second case more flexibility is included and the flight data generated for this case is referred to as FD-AE A/C2.

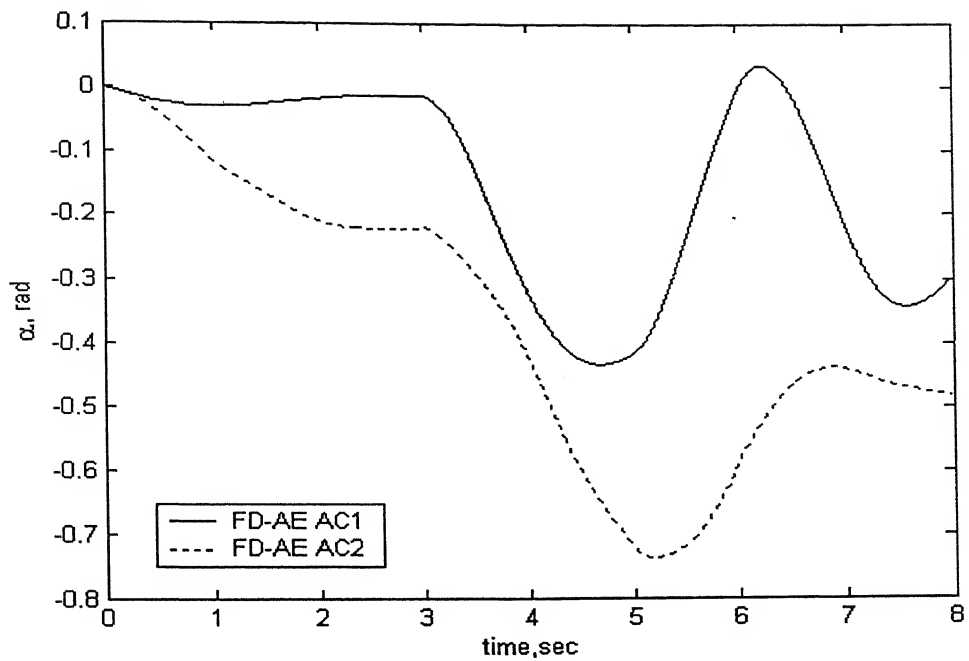


Fig. 3.6 Simulated α response from the flight data FD-AE AC1 and FD-AE AC2

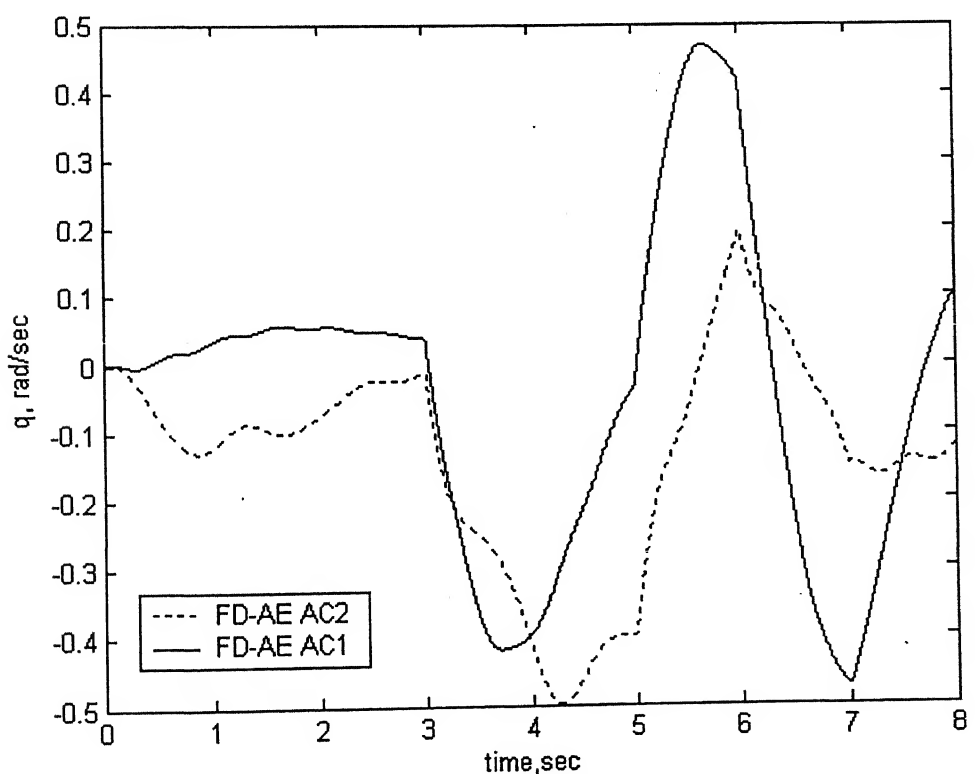


Fig. 3.7 Simulated q response from the flight data FD-AE AC1 and FD-AE AC2.

Table 3.3 Aerodynamic Parameters of the flexible aircraft from Ref. 17

Aerodynamic Parameters							Different generalized displacement coordinates			
							1	2	3	4
C_{x0}	-0.028	C_{L0}	0.34	C_{m0}	-0.252	C_0^{ni}	0.0	0.0	0.0	0.0
$C_{x\alpha}$	0.2005	$C_{L\alpha}$	2.922	$C_{m\alpha}$	-1.66	C_α^{ni}	-148.9e-4	257.8e-4	148.9e-4	334.6e-7
$C_{x\dot{\alpha}}$	0.0	$C_{L\dot{\alpha}}$	0.0	$C_{m\dot{\alpha}}$	-4.3	$C_{\dot{\alpha}}^{ni}$	0.0	0.0	0.0	0.0
C_{xq}	-1.7	C_{Lq}	-14.7	C_{mq}	-34.75	C_q^{ni}	-9.49e-02	1.16e-02	3.97e-02	2.83e-05
$C_{x\delta}$	0.00267	$C_{L\delta}$	0.435	$C_{m\delta}$	-2.578	C_δ^{ni}	-2.24e-04	-1.12e-03	4.46e-04	2.56e-06
C_{xn1}	0.0	C_{Ln1}	0.0288	C_{mn1}	-0.0321	C_{n1}^{ni}	5.85e-05	4.21e-03	2.91e-04	2.21e-05
C_{xn2}	0.0	C_{Ln2}	-0.306	C_{mn2}	-0.025	C_{n2}^{ni}	-9.0e-05	-9.22e-02	1.44e-03	-1.32e-04
C_{xn3}	0.0	C_{Ln3}	-0.0148	C_{mn3}	0.0414	C_{n3}^{ni}	3.55e-04	1.97e-03	-3.46e-04	9.68e-06
C_{xn4}	0.0	C_{Ln4}	0.0140	C_{mn4}	-0.0183	C_{n4}^{ni}	1.20e-04	3.37e-03	1.44e-04	1.77e-03
$C_{x\dot{n}1}$	0.0	$C_{L\dot{n}1}$	0.0848	$C_{m\dot{n}1}$	-0.159	$C_{\dot{n}1}^{ni}$	-4.20e-04	8.71e-03	-6.29e-04	-5.55e-05
$C_{x\dot{n}2}$	0.0	$C_{L\dot{n}2}$	1.03	$C_{m\dot{n}2}$	1.23	$C_{\dot{n}2}^{ni}$	-1.97e-04	-2.98e-01	1.95e-02	4.09e-05
$C_{x\dot{n}3}$	0.0	$C_{L\dot{n}3}$	-0.0608	$C_{m\dot{n}3}$	0.172	$C_{\dot{n}3}^{ni}$	6.50e-04	4.19e-03	-8.77e-06	-4.66e-05
$C_{x\dot{n}4}$	0.0	$C_{L\dot{n}4}$	0.0199	$C_{m\dot{n}4}$	-0.0496	$C_{\dot{n}4}^{ni}$	-1.40e-04	4.15e-03	-1.31e-03	7.99e-02

CHAPTER 4

Results and Discussion

In this chapter, estimated parameters obtained through EKF method are presented.

In the case of ballistic target the factors that affect the behavior of the filter are discussed.

The simulated data corresponding to ballistic target (FD-BT), rigid aircraft (FD-RA) and flexible aircraft (FD-AE AC1 & FD-AE AC2) are used as the measured flight data. The estimated parameters are presented along with their standard deviations to assess the accuracy of the estimates of aerodynamic parameters.

Estimation of Ballistic Coefficient from Flight Data of Ballistic Target (FD-BT)

As mentioned in Chapter 3 the ballistic target is assumed to fall on a straight line path towards the surface based tracking radar. The ballistic coefficient (β) is estimated through EKF method. It has been observed that there is a negligible change in the estimated value of β by the increase of terms in the Taylor series expansion for the approximation of fundamental matrix $[\phi_k]$ in Eq. A.10 of Appendix A. This is valid because the fundamental matrix is actually an infinite Taylor series expansion of the product of sampling time t_s and system dynamics matrix $[F]$.

Table 4.1 Estimated ballistic coefficient without process noise

	True Value	Estimated Value by 2 terms	Estimated Value by 3 terms
Ballistic Coefficient β (Lb/Ft/sec ²)	500	497.8827 (0.290904)*	499.8196 (0.290046)*

* Standard Deviation

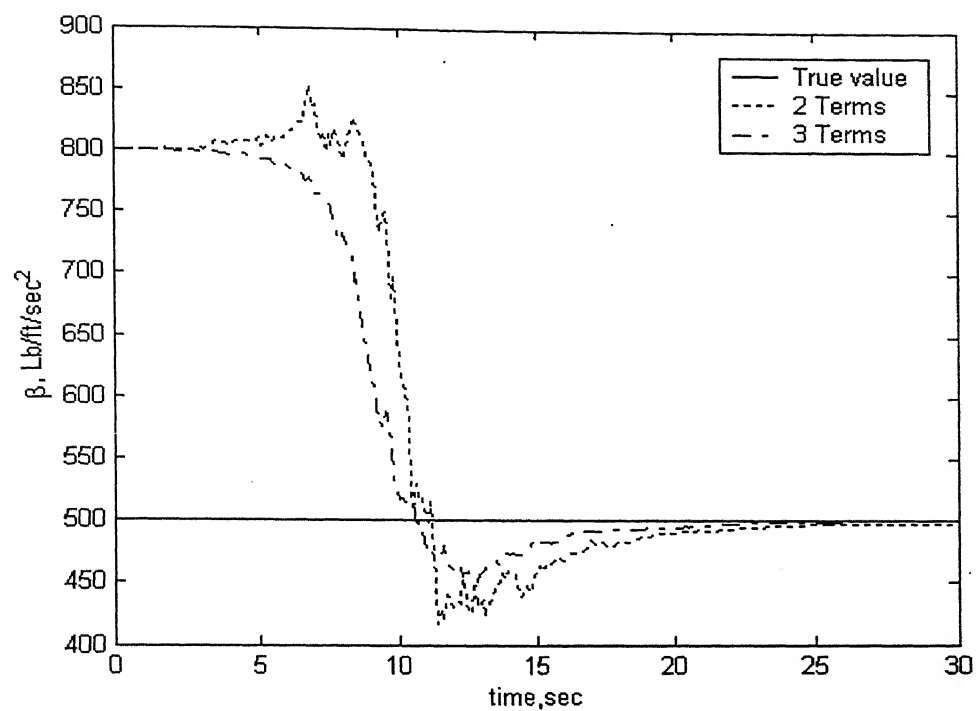


Fig. 4.1 Estimation of ballistic coefficient β without process noise

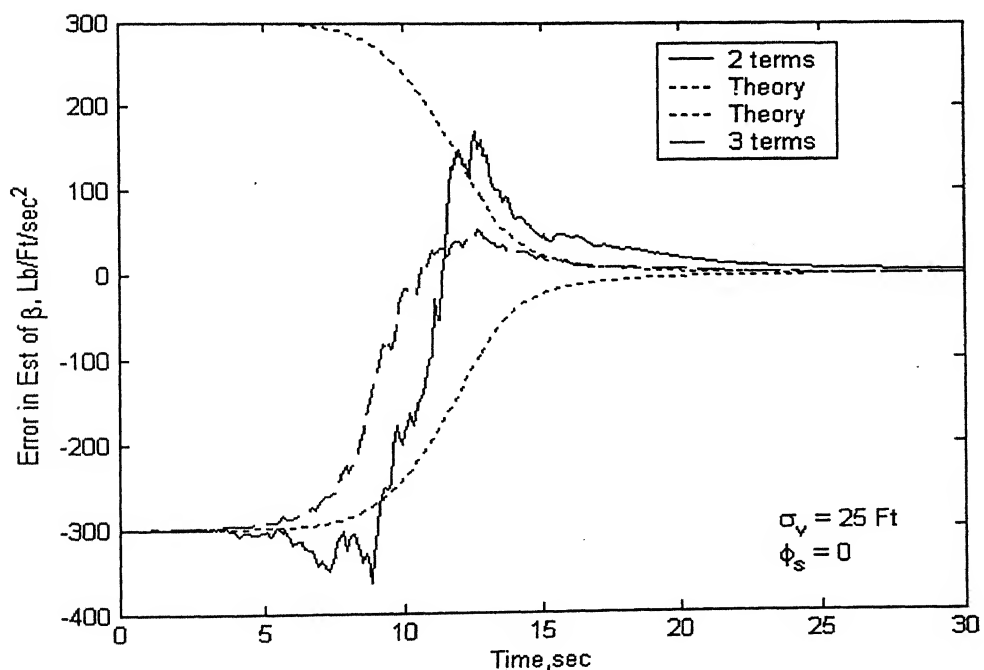


Fig. 4.2 Error in the estimation of ballistic coefficient β without process noise

For the same case the process noise is included assuming that the filter's knowledge of the real world is in error. It has been observed that addition of process noise to the filter increases the errors in the estimates. Also there is not much difference by increase of number of terms in the Taylor series expansion for the approximation of fundamental matrix $[\phi_k]$. From the Table. 4.1 and Table. 4.2 it is evident that by including process noise the accuracy in the estimates deteriorated. Similar observation can be made by comparing Fig. 4.1 and Fig. 4.2 with Fig. 4.3 and Fig. 4.4.

Table 4.2 Estimation of ballistic coefficient with process noise

	True Value	Estimated Value by 2 terms	Estimated Value by 3 terms
Ballistic Coefficient β (Lb/Ft/sec ²)	500	488.9278 (11.07214)	488.7636 (11.23639)

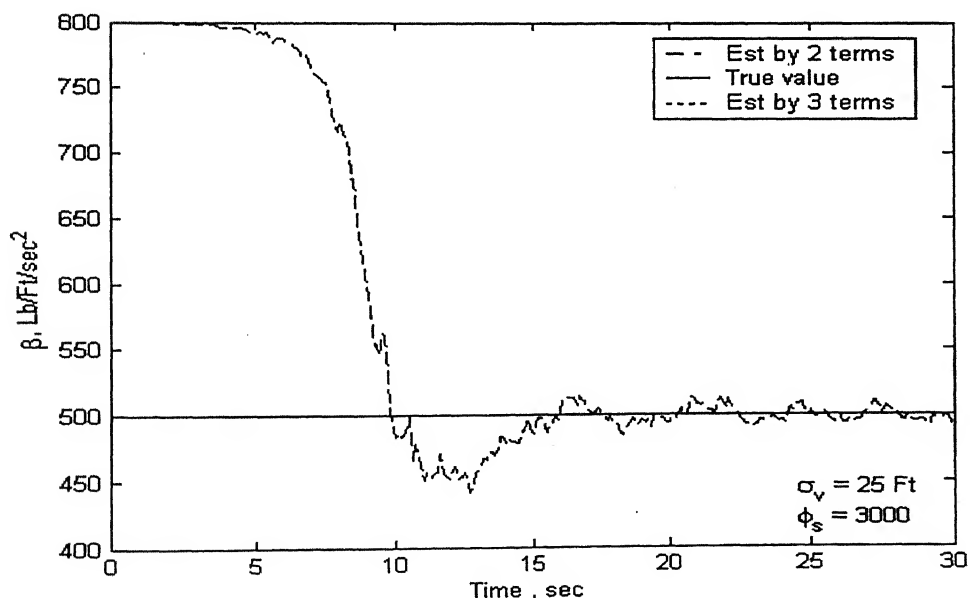


Fig. 4.3 Estimation of ballistic coefficient β with process noise

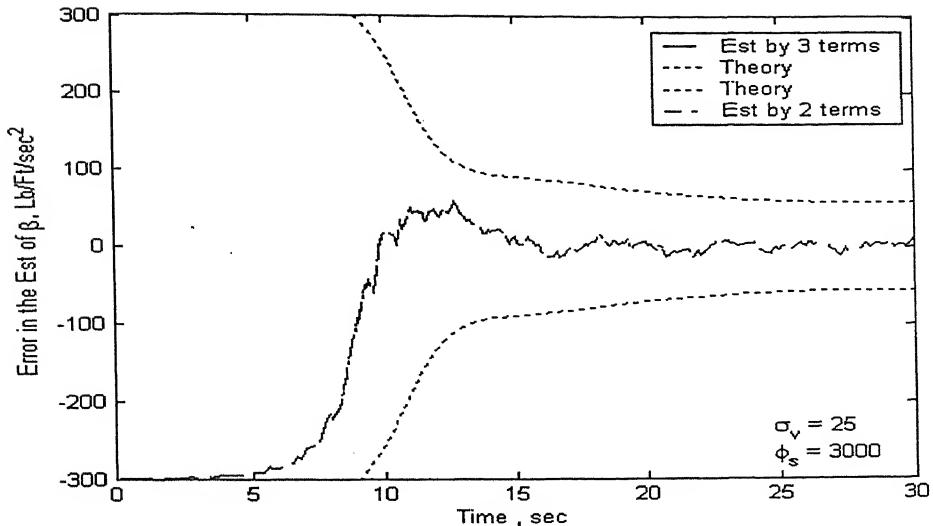


Fig. 4.4 Error in the estimation of ballistic coefficient β with process noise

Estimation of Aerodynamic Parameters from Flight Data of Rigid Aircraft (FD-RA/C)

Knowledge of aerodynamic parameters is of paramount importance, to develop accurate mathematical model which represents the longitudinal dynamics of an aircraft. The aerodynamic parameters needed to develop the aerodynamic model are force derivatives $C_{L\alpha}$, C_{Lq} , $C_{L\delta_e}$ and pitching moment derivatives $C_{m\alpha}$, C_{mq} , $C_{m\delta_e}$. Thus, a study was carried out to explore the possibility of extracting the parameters using EKF method. The simulated data generated, FD-RA/C of the example aircraft is added with Gaussian noise and is used as the measured data in the EKF algorithm. The six aerodynamic parameters $C_{L\alpha}$, C_{Lq} , $C_{L\delta_e}$, $C_{m\alpha}$, C_{mq} and $C_{m\delta_e}$ are considered as state variables along with the flight variables, α and q . The algorithm is run for an elevator input 3-2-1-1 for 8 seconds and the estimated aerodynamic parameters are tabulated along with their standard deviations in Table. 4.3. The measurement noise variance is

0.016 for both α and q . In Case A the values of diagonal elements of process noise matrix are same and are randomly chosen to be 0.008 and in Case B the values are differently chosen as an attempt to tune process noise.

Table. 4.3 Estimated Aerodynamic Parameters from FD-RA/C

Case	Aerodynamic Parameters					
	$C_{L\alpha}$	C_{Lq}	$C_{L\delta_e}$	$C_{m\alpha}$	C_{mq}	$C_{m\delta_e}$
True Values	2.922	-14.7	0.435	-1.66	-34.75	-2.578
No Process Noise	2.9096 (0.00764)	-22.7217 (0.75708)	0.6756 (0.01976)	-1.6078 (0.00166)	-38.3583 (6.68809)	-2.5619 (0.00289)
Process Noise Case A	2.8772 (0.06228)	-16.6971 (1.78776)	-0.3212 (0.13688)	-1.8501 (0.03303)	-39.0636 (6.9463)	-2.7122 (0.10493)
Process Noise Case B	2.8887 (0.08767)	-16.8602 (1.89439)	-0.2328 (0.14417)	-1.6099 (0.0784)	-41.527 (6.94662)	-2.8064 (0.0588)

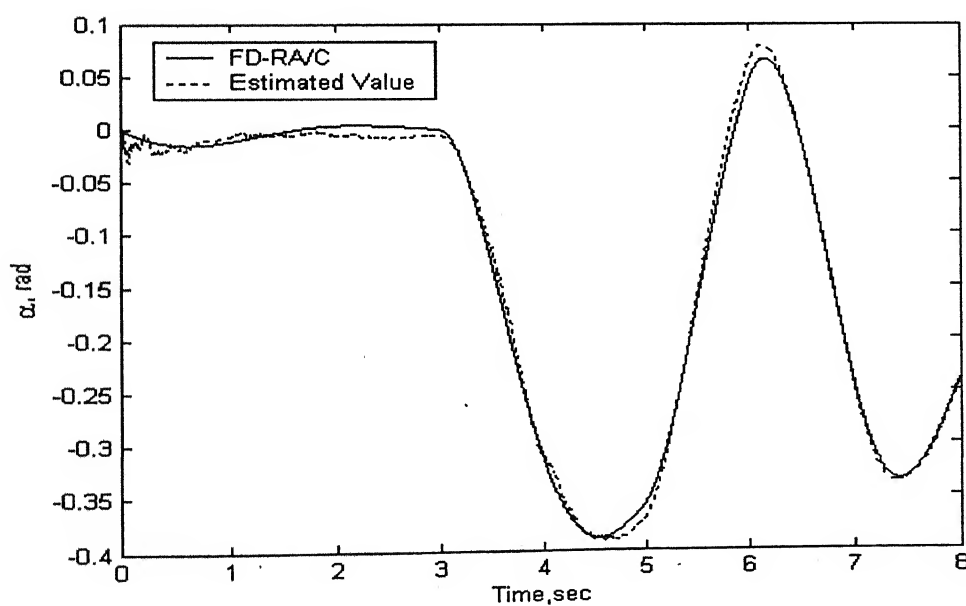


Fig. 4.5 Comparison of the estimated α value with that of FD-RA/C

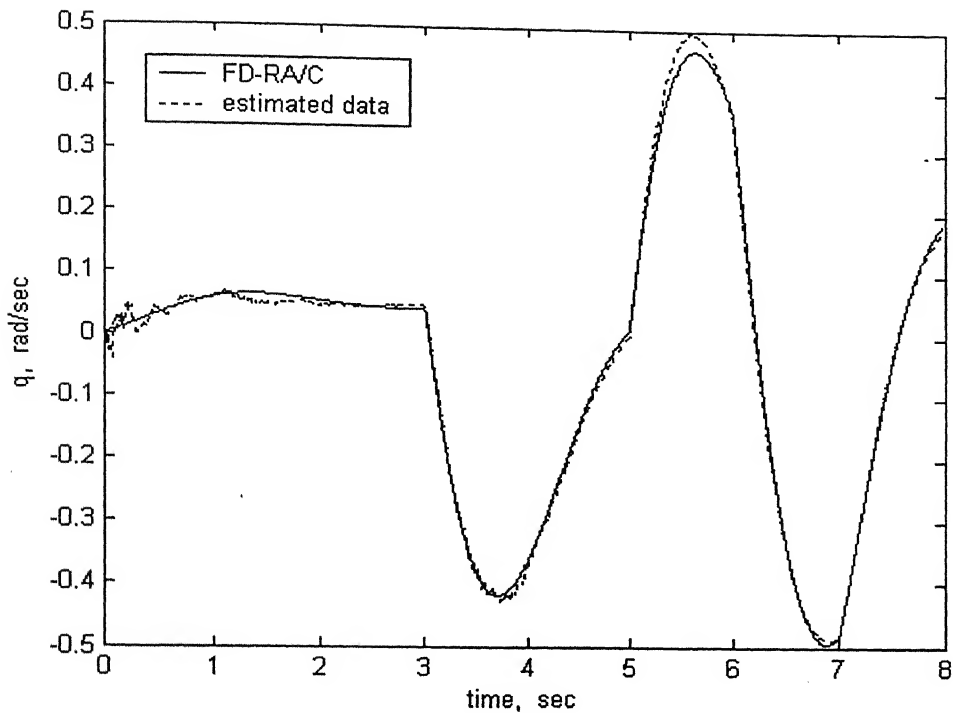


Fig . 4.6 Comparison of the estimated q value with that of FD-R/A/C.

Through the values listed in Table 4.3 it can be observed that by including process noise the estimated parameters show large variance however we can also infer that by proper choice of noise values the estimate of parameters can be improved.

Estimation of Equivalent Aerodynamic Parameters from Flight Data of Flexible Aircraft (FD-AE A/C1 & FD-AE A/C2)

The simulated data from FD-AE A/C1 and FD-AE A/C2 is used in the EKF algorithm by adding Gaussian noise to the data. All the 4 elastic modes of the test aircraft are considered in the generation of the simulated data. A full order model of an aeroelastic aircraft has too many parameters to yield satisfactory estimates using any of the conventional parameter estimation methods. In view of this, a study was carried out to identify a simplified model with reduced number of parameters, and to evaluate how the

resulting parameters are affected by model simplifications. To start with, a rigid body model was assumed and parameters were estimated from flight data that contain the aeroelastic effects. It is expected that the parameter estimates thus obtained would absorb the aeroelastic effects. For the convenience of discussion, these parameters are referred by ‘equivalent parameters’ in Ref. 19. An analytical expression has been proposed to analytically compute the numerical values of the equivalent parameters. It is shown that the numerical value of analytical expression indicates the degree of flexibility of the aircraft, and thereby, a criterion based on it is suggested for deciding adequacy or otherwise of using simpler rigid body models in estimation algorithm. In the EKF algorithm only aerodynamic parameters $C_{L\alpha}, C_{Lq}, C_{L\delta_e}, C_{m\alpha}, C_{mq}$ and $C_{m\delta_e}$ are estimated and presented in Table. 4.4.

Table 4.4 Equivalent Aerodynamic Parameters from FD-AE A/C1 and FD-AE A/C2

	Equivalent Aerodynamic Parameters					
	$C_{L\alpha}$	C_{Lq}	$C_{L\delta_e}$	$C_{m\alpha}$	C_{mq}	$C_{m\delta_e}$
True Values	2.922	-14.7	0.435	-1.66	-34.75	-2.578
FD-AE A/C1	2.4927 (0.006445)	-1.5588 (0.6973)	0.9644 (0.0179)	-1.3141 (0.0012)	-20.6907 (6.6134)	-2.2514 (0.00271)
FD-AE A/C2	1.7955 (0.017004)	-7.7374 (2.56618)	-0.2195 (0.06234)	-0.4582 (0.001378)	-15.2807 (6.932)	-1.5197 (0.00752)

The equivalent aerodynamic parameters are in close agreement with values presented in Ref. 19. For the case of FD-AE A/C 1 the measurement noise for α and q is 0.016 but for the case of FD-AE A/C 2 the measurement noise is 0.09. For the case of FD-AE A/C

2 the aeroelastic effects of more flexible aircraft are got included in the algorithm as measurement noise.

Estimation of Aerodynamic Parameters from Flight Data of Flexible Aircraft (FD-AE A/C1 & FD-AE A/C2)

In the final case both the flight data FD-AE A/C1 and FD-AE A/C2 are processed by the EKF algorithm. The algorithm includes only 15 parameters, taking into account only the first elastic mode. Along with the flight variables α and q the generalized displacement coordinate η_1 and its derivative $\dot{\eta}_1$ are also taken as the state variables. The estimated values of aerodynamic parameters are presented in Table. 4.5. It is seen that the estimation deteriorates as the flexibility increases. Thus for high flexibility aircraft such an approximation may not yield better results Comparison of estimated response of α , q with that of the flight data FD-AE AC1 and FD-AE AC2 are presented pictorially in Fig.4.7 to Fig. 4.10. Based on these Fig. 4.7 to Fig. 4.10 it can be easily seen that the estimated response (α, q) closely matches with the simulated response. However, there is a large difference between these parameters; it can be used for simulators and control law specifications to initiate the analysis.

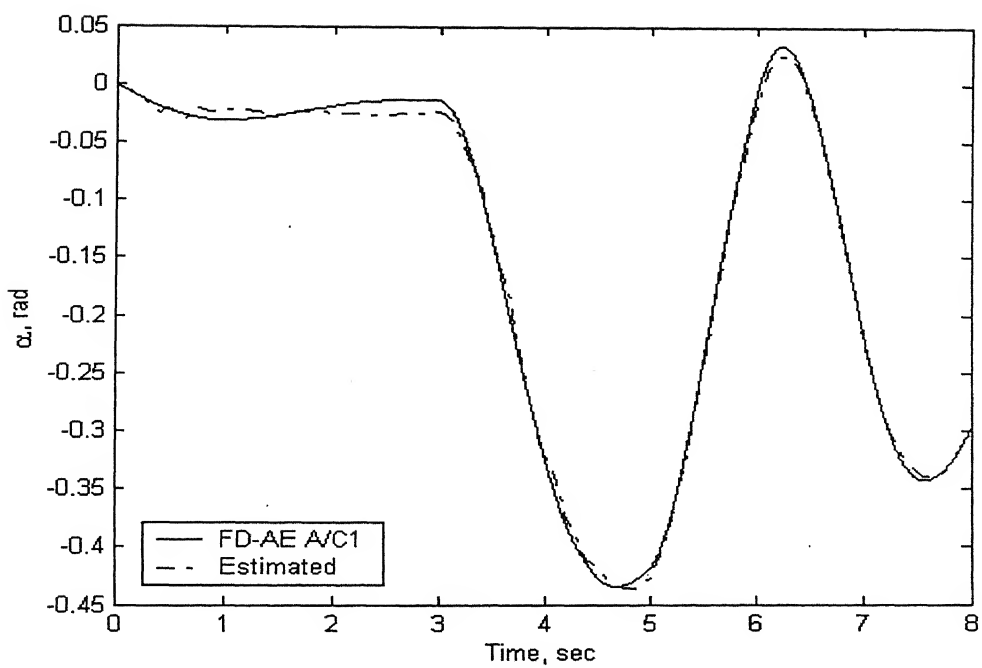


Fig . 4.7 Comparison of estimated value of α with that of FD-AE A/C1

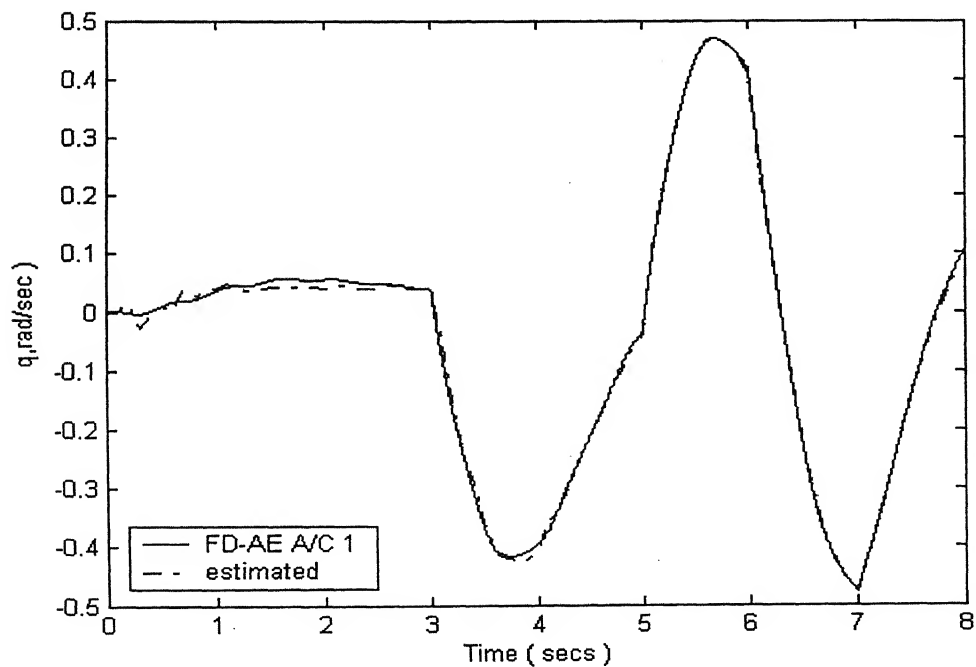


Fig . 4.8 Comparison of estimated value of q with that of FD-AE A/C1

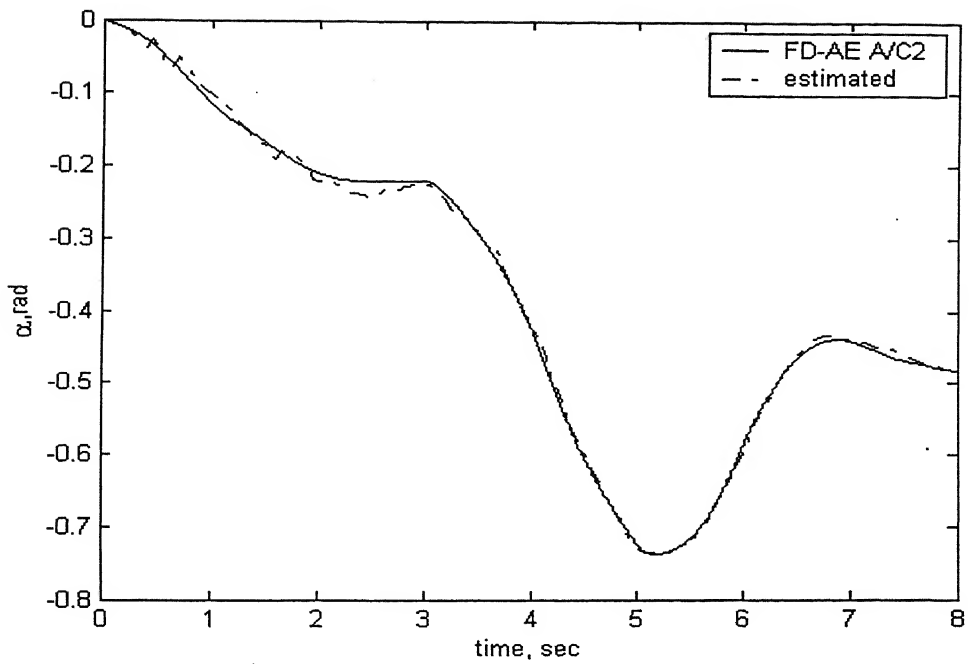


Fig . 4.9 Comparison of estimated value of α with that of FD-AE A/C2

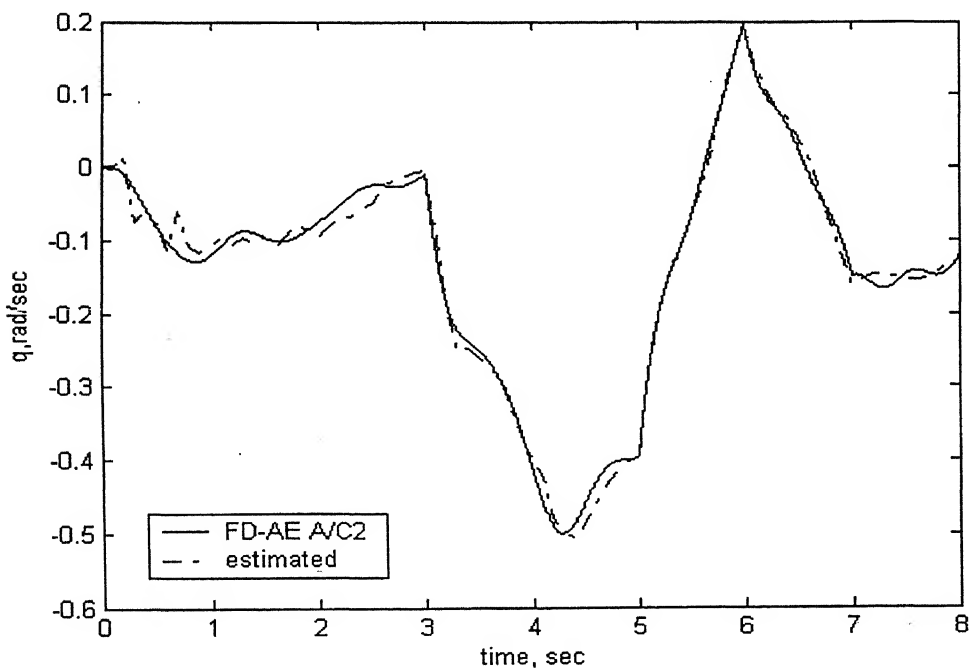


Fig . 4.10 Comparison of estimated value of q with that of FD-AE A/C2

Table 4.5 Estimated Aerodynamic Parameters from flight data FD-AE AC1 and FD-AE AC2

	True Values	FD-AE AC1	FD-AE AC2
C_{L_α}	2.922	3.2861 (0.0445)	3.0798 (0.03598)
C_{L_q}	-14.7	-13.2036 (1.02)	-24.6586 (1.7327)
$C_{L_{\delta_e}}$	0.435	0.8184 (0.0312)	0.2619 (0.03821)
C_{m_α}	-1.66	-1.6082 (0.0084)	-1.8725 (0.01857)
C_{m_q}	-34.75	-32.4563 (0.2808)	-41.1266 (0.49461)
$C_{m_{\delta_e}}$	-2.578	-2.565 (0.0145)	-2.1175 (0.01376)
$C_{L_{\eta_1}}$	0.0288	0.0556 (0.0024)	0.012 (0.000479)
$C_{L_{\dot{\eta}_1}}$	0.0848	0.0905 (0.0163)	0.1792 (0.01244)
$C_{m_{\eta_1}}$	0.0025	-0.0411 (0.0025)	-0.0201 (0.000129)
$C_{m_{\dot{\eta}_1}}$	-0.159	-0.0799 (0.022)	-0.1873 (0.00451)
$C_{\eta_1 \alpha}$	-0.014898	-0.017 (0.0018)	-0.0244 (0.000281)
$C_{\eta_1 q}$	-0.0949	-0.1 (0.0186)	-0.0672 (0.009936)
$C_{\eta_1}^{\eta_1}$	0.0000585	0.000062 (0.00001)	0.000126 (0.000002)
$C_{\dot{\eta}_1}^{\eta_1}$	-0.00042	-0.000587 (0.00007)	-0.000842 (0.000027)
$C_{\delta_e}^{\eta_1}$	-0.012835	-0.0127 (0.0012)	-0.009864 (0.000217)

CHAPTER 5

Conclusion and Suggestions For Future Work

5.1 Conclusion

In the present work, EKF method has been applied to estimate aerodynamic parameters from simulated flight data. The method has been applied starting from flight data of a one-dimensional ballistic target to flight data of a rigid aircraft and then to the flight data of a flexible aircraft. It is observed that EKF method can be applied successfully to estimate the parameters from the flight data of the three cases. The method also estimates equivalent aerodynamic parameters in which aeroelastic effects get absorbed. If appropriate mathematical model of the system is provided then the method can be used advantageously to estimate force and moment derivatives.

5.2 Suggestions for future work

1. Due to non-availability of real flight data, aerodynamic parameters were estimated using simulated flight data. In order to enhance the proposed schemes, these parameters should be validated using real flight data.
2. All the simulated data is generated under standard atmospheric conditions. Applicability of the proposed schemes to estimate parameters under non-standard atmospheric conditions can be explored.
3. To obtain reliable results from recursive techniques like EKF, it becomes necessary to tune the filter parameters fairly well offline before implementing the technique online. Proper filter tuning methods like Tapley Meyer's algorithm¹⁶ or Adaptive Kalman filtering¹⁴ can be applied to tune the process noise and measurement noise characteristics.

APPENDIX -A

Kalman filter design for Ballistic Target

The ballistic coefficient of the object is unknown and it is made one of the states and also it is assumed that the ballistic coefficient is constant. The states for the proposed filter are given by

$$[X] = \begin{bmatrix} x \\ \dot{x} \\ \beta \end{bmatrix} \quad (A.1)$$

The complete set of equations required to build the filter are

$$\ddot{x} = \frac{0.0034g_B e^{-x/22000}}{2\beta} - g_B \quad (A.2)$$

$$\dot{\beta} = 0 \quad (A.3)$$

The resultant filter can be made more robust by adding process noise to the derivative of the ballistic coefficient. Then the derivative of the ballistic coefficient becomes

$$\dot{\beta} = u_s \quad (A.4)$$

The two differential equations Eq. (A.2) and Eq. (A.3) can be linearised as follows

$$\begin{bmatrix} \Delta\dot{x} \\ \Delta\ddot{x} \\ \Delta\dot{\beta} \end{bmatrix} = \begin{bmatrix} \frac{\partial \dot{x}}{\partial x} & \frac{\partial \dot{x}}{\partial \dot{x}} & \frac{\partial \dot{x}}{\partial \beta} \\ \frac{\partial \ddot{x}}{\partial x} & \frac{\partial \ddot{x}}{\partial \dot{x}} & \frac{\partial \ddot{x}}{\partial \beta} \\ \frac{\partial \dot{\beta}}{\partial x} & \frac{\partial \dot{\beta}}{\partial \dot{x}} & \frac{\partial \dot{\beta}}{\partial \beta} \end{bmatrix} \begin{bmatrix} \Delta x \\ \Delta \dot{x} \\ \Delta \beta \end{bmatrix} + \begin{bmatrix} 0 \\ 0 \\ u_s \end{bmatrix} \quad (A.5)$$

For the present case it is assumed that the ballistic coefficient is constant and so u_s is zero.

The systems dynamics matrix is the matrix of partial derivatives and is given by

$$[F] = \begin{bmatrix} \frac{\partial \dot{x}}{\partial x} & \frac{\partial \dot{x}}{\partial \dot{x}} & \frac{\partial \dot{x}}{\partial \beta} \\ \frac{\partial \ddot{x}}{\partial x} & \frac{\partial \ddot{x}}{\partial \dot{x}} & \frac{\partial \ddot{x}}{\partial \beta} \\ \frac{\partial \dot{\beta}}{\partial x} & \frac{\partial \dot{\beta}}{\partial \dot{x}} & \frac{\partial \dot{\beta}}{\partial \beta} \end{bmatrix}_{x=\hat{x}} \quad (\text{A.6})$$

The partial derivatives are evaluated at the current state estimates. The system dynamics matrix of the present case turns out to be

$$[F] = \begin{bmatrix} 0 & 1 & 0 \\ \frac{-\hat{\rho}_B g_B \hat{x}^2}{44,000 \hat{\beta}} & \frac{\hat{\rho}_B g_B \hat{x}}{\hat{\beta}} & \frac{-\hat{\rho}_B g_B \hat{x}^2}{2\hat{\beta}^2} \\ 0 & 0 & 0 \end{bmatrix}_{x=\hat{x}} \quad (\text{A.7})$$

For simplification the following terms are introduced

$$f_{21} = \frac{-\hat{\rho}_B g_B \hat{x}^2}{44,000 \hat{\beta}} \quad (\text{A.8.1})$$

$$f_{22} = \frac{\hat{\rho}_B g_B \hat{x}}{\hat{\beta}} \quad (\text{A.8.2})$$

$$f_{23} = \frac{-\hat{\rho}_B g_B \hat{x}^2}{2\hat{\beta}^2} \quad (\text{A.8.3})$$

The system dynamics matrix transforms to

$$[F] = \begin{bmatrix} 0 & 1 & 0 \\ f_{21} & f_{22} & f_{23} \\ 0 & 0 & 0 \end{bmatrix} \quad (\text{A.9})$$

The fundamental matrix $[\phi(t)]$ is found by the Taylor-series approximation and is given by the equation

$$[\phi(t)] = [I] + [F]t + \frac{[F]^2 t^2}{2!} + \frac{[F]^3 t^3}{3!} + \dots \quad (\text{A.10})$$

Since the fundamental matrix is only used in the Riccati equations the first two terms of the Taylor-series expansion is considered to obtain the fundamental matrix. Also by the increase in number of terms there may not necessarily be a considerable change in the estimate of the states.

$$[\phi(t)] \approx [I] + [F]t = \begin{bmatrix} 1 & t & 0 \\ f_{21}t & 1 + f_{22}t & f_{23}t \\ 0 & 0 & 1 \end{bmatrix} \quad (\text{A.11})$$

The discrete fundamental matrix is obtained by substituting T_s for t and is given by

$$[\phi_k] \approx \begin{bmatrix} 1 & T_s & 0 \\ f_{21}T_s & 1 + f_{22}T_s & f_{23}T_s \\ 0 & 0 & 1 \end{bmatrix} \quad (\text{A.12})$$

In the example considered the altitude measurement is a linear function of the states and is given by

$$\dot{x}^* = [1 \ 0 \ 0] \begin{bmatrix} x \\ \dot{x} \\ \beta \end{bmatrix} + v \quad (\text{A.13})$$

where v is the measurement noise. By inspection of the measurement equation we can get the measurement matrix $[H]$ and the discrete measurement noise matrix $[R]$

$$[H] = [1 \ 0 \ 0] \quad (\text{A.14})$$

$$R_k = E(v_k v_k^T) \quad (\text{A.15})$$

The discrete measurement noise matrix for the problem considered turns out to be a scalar and is given by the equation

$$R_k = \sigma_v^2 \quad (\text{A.16})$$

If the resultant filter needs to be more robust then process noise can be included. The continuous process noise matrix $[Q]$ is given by

$$[Q] = \begin{bmatrix} 0 & 0 & 0 \\ 0 & 0 & 0 \\ 0 & 0 & \phi_s \end{bmatrix} \quad (\text{A.17})$$

where ' ϕ_s ' is the spectral density of the white noise source assumed to be on the derivative of the ballistic coefficient .The discrete process noise matrix $[Q]$ is derived from the continuous process-noise matrix according to the expression

$$[Q_k] = \int_0^{T_s} [\phi(\tau)] [Q] [\phi^T(\tau)] d\tau \quad (\text{A.18})$$

After integration the final expression for the discrete process noise matrix is given by the expression

$$[Q_k] = \begin{bmatrix} 0 & 0 & 0 \\ 0 & f_{23}^2 \frac{T_s^3}{3} & f_{23} \frac{T_s^2}{3} \\ 0 & f_{23} \frac{T_s^2}{2} & T_s \end{bmatrix} \quad (\text{A.19})$$

The Kalman-filtering equations are written as

$$\hat{x}_k = \bar{x}_k + K_{1_k} (x_k^* - \bar{x}_k) \quad (\text{A.20.1})$$

$$\hat{\dot{x}}_k = \bar{\dot{x}} + K_{2_k} (x_k^* - \bar{x}_k) \quad (\text{A.20.2})$$

$$\hat{\beta}_k = \hat{\beta}_{k-1} + K_{3_k} (x_k^* - \bar{x}_k) \quad (\text{A.20.3})$$

The three-state extended Kalman filter and Riccati equations were programmed, along with the simulation of the real world. The process noise matrix is set to zero assuming β to be a constant. The third element of the initial covariance matrix is set to 300^2 some

guess value to reflect the uncertainty in the initial guess at the estimated ballistic coefficient. The initial states of the filter are chosen close to the true values. The altitude state x is in an error by 25 ft and the velocity state \dot{x} is in an error by 150 ft/s. The initial covariance matrix reflects the errors in the position state and the velocity state.

References

1. Hamel , P . G., "Aircraft Parameter Identification Methods and their Applications Survey and Future Aspects," AGARD, 15 –104, Nov .1979, Paper 1.
2. Maine, R.E. and Iliff, K.W., "Identification of Dynamic System-theory and Formulations", NASA RP 1138, Feb 1985.
3. Klein, V., "Estimation of Aircraft Aerodynamic parameter from Flight Data," progress in Aerospace Sciences, Vol. 26, 1989, pp. 1-77.
4. Brayan, G . H . , Stability in Aviation, Mc Millan, London, 1911.
5. Peter G. Hamel and Jategaonkar, R . V . , "The Evolution of Flight Vehicle System Identification, "AGARD, DLR Germany, 8-10, May, 1995.
6. Milliken, W . F . , "Progress in Dynamic Stability and Control Research," Journal of Aeronautical Sciences, Vol. 14, No. 9, 1947, pp. 493-519.
7. Shinbort, M., "A Least Square Curve Fitting Method with Applications to the Calculation of Stability Coefficients from Transient Response Data," NACA TN-2341.
8. Zarchan, P. and Musoff, H, "Fundamentals of Kalman Filtering" , Progress in Astronautics and Aeronautics, Volume 190, AIAA Sept 2000.
9. Pietrass, A. "Determination of Aerodynamic Derivatives of the FIAIA G9 IT3 Aircraft from Flight Test by means of Manual Analog Model Matching", Paper No. N75-19257 of Publication ESRO TT-104, Nov 1974.
10. Taylor, L. W., Iliff, K.W. and Powers, B.G. "A comparison of Newton-Raphson and other methods for Determining Stability Derivatives from Flight Data", AIAA Paper No. 69-315, May 1969.
11. Peter S. Maybeck. , "Stochastic Models, Estimation, and Control", Vol. 1, Academic Press, New York, 1979.
12. Kalman, R.E., "A New Approach to Linear Filtering and Prediction Problems", Transactions of the American Society of Mechanical Engineers, Series D, Journal of Basic Engineering, Vol. 82, March 1960, pp.35-45.
13. Jategaonkar, R . V ., Plaetschke, E., " Algorithms for Aircraft parameter Estimation Accounting for Process and Measurement Noise", Journal of Aircraft, Vol.26, No.4.1989,pp. 360-372.

14. Mehra, R., "On the identification of variances and Adaptive Kalman filtering", IEEE transactions on Automatic Control, Vol. AC-15, No.2, 1970, pp.175-184.
15. Morelli, E., "Estimating noise Characteristics from Flight Test Data Using Fourier Smoothing", AIAA Paper 94-0152, Jan. 1994.
16. Myers, K.A., Tapley, B.D., "Adaptive sequential estimation with Unknown Noise Statistics", IEEE Transactions on Automatic Control, Vol. Ac 21, 1976, pp 520-525.
17. Martin, R. W. and David. K .S. "Flight Dynamics of Aeroelastic Vehicles", Journal of Aircraft, Vol. 25, No.6, June 1988.
18. Grewal, M.S., Andrews, A.S., "Kalman Filtering-Theory and Practice Using MATLAB", Second Edition, John Wiley & Sons, 2001.
19. Ghosh, A . K., "Aircraft Parameter Estimation from Flight Data using Feed Forward Neural Networks", Ph.D Thesis, Department of Aerospace Engineering, IIT Kanpur, April 1998.
20. Zhou, J. and Luecke, H. R., "Estimation of the Covariance of the Process Noise and Measurement Noise for a Linear Discrete Dynamic System", Journal of Computers Chemical Engineering, Vol. 19, No. 2, pp. 187-195,1995.
21. Chandrasekhar, K .V., "On Application of Maximum Likelihood Method and Kalman-Filter Technique to Estimate Parameters from Flight Data of Rockets and Shells", M.Tech. Thesis, Department of Aerospace Engineering, IIT Kanpur, June 2004.
22. Nelson, "Flight Stability and Automatic Control", Second Edition, Mc-Graw Hill,1997.